SANDIA REPORT

3/20/96

Influence of Pore Pressure and Production-Induced Changes in Pore Pressure on In Situ Stress

RECEIVED

APR 0 3 1996

O S T I

Lawrence W. Teufel

Approved for public release; distribution is unlimited.

SF2900Q(8-81)

MASTER

Influence of Pore Pressure and Production-Induced Changes in Pore Pressure on In Situ Stress

Lawrence W. Teufel*
Geomechanics Department
Sandia National Laboratories
Albuquerque, NM 87185-0751
(*Current address: University Partnership
Regional Office at New Mexico Tech
Sandia National Laboratories
Socorro, New Mexico 87801)

ABSTRACT

Knowledge of in situ stress and how stress changes with reservoir depletion and pore pressure drawdown is important in a multi-disciplinary approach to reservoir characterization, reservoir management, and improved oil recovery projects. This report summarizes a compilation of in situ stress data from six fields showing the effects of pore pressure and production-induced changes in pore pressure on the minimum horizontal stress. The in situ stress data and corresponding pore pressure data were obtained from field records of the operating companies and published reports. Horizontal stress was determined from closure pressure data of hydraulic fractures and leak-off tests. The stress measurements clearly demonstrate that the total minimum-horizontal stress is dependent on pore pressure. A decrease in pore pressure either by geologic processes or production of a reservoir will result in a decrease in the total minimum-horizontal stress. The magnitude of changes in stress state with net changes in pore pressure is dependent on local field conditions and cannot be accurately predicted by the uniaxial strain model that is commonly used by the petroleum industry.

TABLE OF CONTENTS

1. INTRODUCTION

In situ stress affects nearly all physical properties of rock and hence the measurement and interpretation of (1) geophysical data, (2) petrophysical properties such as porosity and permeability, (3) rock strength and ductility, and (4) mechanisms of rock deformation and failure. In naturally fractured reservoirs, the influence of stress on reservoir behavior is even more pronounced, particularly with respect to fluid flow through fractures. Accordingly, knowledge of in situ stress is becoming increasingly important in current trends toward a multi-disciplinary approach to reservoir characterization, reservoir management, and in the development and completion of oil and gas reservoirs. Some important examples include reservoir compaction during fluid withdrawal, behavior of natural fractures, hydraulic fracture growth, interaction between natural and induced hydraulic fractures, fracturing during waterflooding, and wellbore stability.

Knowledge of the in situ stress state at depth is not easily obtained. Various models have been proposed to calculate in situ stresses and depend on a complex history of properties and loading conditions (Voight, 1974; Rosepiler, 1979; Prats, 1981; Warpinski, 1989). Application of these models is limited because of the large uncertainty in mechanical properties of large rock masses and loading conditions in the subsurface.

The model most commonly used by the petroleum industry is the elastic uniaxial strain model (Hubbert and Willis, 1957). This simple model predicts the total horizontal stress from a knowledge of the overburden stress, pore pressure, and Poisson's ratio and is given by:

$$S_{Hmax} = S_{Hmin} = (\upsilon / (1-\upsilon)) (S_v - \alpha P) + \alpha P$$

where S_{Hmax} and S_{Hmin} are the total maximum and minimum horizontal stresses, S_v is the total vertical or overburden stress, υ is Poisson's ratio, and α is a poroelastic parameter. For this elastic model the horizontal stresses are dependent only on gravitational loading. The model assumes no lateral displacement during deformation (zero horizontal strain boundary condition). Horizontal stresses are equal, increase with depth, and change with changes in pore pressure or Poisson's ratio (due to changes in lithology).

Although the uniaxial strain model is relatively simple, it clearly shows that for gravitational loading the pore pressure directly affects the magnitude of the horizontal stresses. Changes in pore pressure over geologic time or during the production of a reservoir will change the horizontal stress state. This means that measurements of horizontal stress must include measurements of the pore pressure in order to compare stress data from different locations or through time.

Several different techniques have been developed to measure or infer the orientation and magnitude of principal horizontal stresses at depth. These include (1)

hydraulic fracture stress tests (Kehle, 1961; Warpinski et al, 1985), leak-off tests (Kunze and Steiger,1992), (2) various core analyses such as anelastic strain recovery (Teufel, 1983; Warpinski and Teufel, 1989), differential strain curve analysis (Ren and Roegiers, 1983), differential wave velocity analysis (Ren and Hudson, 1985), and (3) wellbore condition logs (such as televiewers and four-arm calipers) to examine the eccentricity and breakouts (Bell and Gough, 1982).

The objective of this report is to provide a compendium of in situ stress data from six oil and gas fields that shows the influence of pore pressure and production-induced changes in pore pressure with reservoir depletion on horizontal stress. The six fields include the (1) Valhall Field, North Sea- chalk reservoir (2) Eldfisk Field, North Sea - chalk reservoir (3) Ekofisk Field, North Sea - chalk reservoirs and overburden rock, (4) Oseberg Field, North Sea - overburden rock, (5) McAllen Ranch Field, Texas - sandstone reservoirs, and (6) Rulison Field, Colorado - sandstone reservoirs. Minimum horizontal stress was determined from closure pressure data of hydraulic fractures and leak-off tests. These data were obtained from records of the operating companies of the fields and published reports.

2. TECHNIQUES FOR MEASURING IN SITU STRESS AT DEPTH

In this report we will only present minimum horizontal stress data estimated from closure pressure data of hydraulic fracture and leak-off tests. A brief description of the two techniques as used by the petroleum industry follows.

2a. Hydraulic Fracture Method

Hydraulic fracturing is a standard method used by the petroleum industry to estimate the minimum horizontal stress magnitude in cased and perforated holes. The most accurate procedure is to conduct small-volume hydraulic fractures, which is discussed in detail by Warpinski et al. (1985). Briefly, this procedure consists of (1) perforating a 0.6 m interval with eight perforations, (2) isolating the interval with straddle packers, (3) fracturing the rock with small volumes 0.04 to 0.4 m^3 of KCL water and recording the pressure with a bottomhole, quartz pressure gage, (4) shutting in with a downhole closure tool, and (5) determining the instantaneous-shut-in-pressure (ISIP), which for small volume tests with low-viscosity fluid, is essentially the minimum horizontal stress. The major uncertainty with this technique is the ability to obtain, measure, and interpret a clear ISIP. Because the test is conducted in a cased and perforated hole, no information on the maximum horizontal stress or the stress orientation can be obtained.

Fracture closure pressure data from small volume hydraulic fractures presented by Warpinski and Teufel (1989) were used to estimate the influence of pore pressure on minimum horizontal stress of Mesaverde sandstones in the Rulison Field, Colorado. Figure 1 shows example stress-test pressure data for representative sandstones from Warpinski and Teufel (1989). The nominal injection rate for these tests is 0.44 L/s. The

pressure records are characterized by a relatively high injection pressure and a large pressure drop at shut-in. The ISIP is well defined even with the large drop in pressure at shut-in.

Small-volume hydraulic-fracture stress tests are not commonly conducted by the industry because they are expensive. However, larger volume hydraulic fracture treatments can, in some cases, be used to infer the minimum horizontal stress magnitude. These treatments are made in selected perforated intervals. The perforated zones are usually short discontinuous intervals of less than 15 m. The gross vertical height of all perforated zones that are fractured can range up to 150 m. The first phase of a large fracture treatment is to inject 25 to 55 m^3 of KCL water or sea water into the well to breakdown the formation and then the well is shut-in before the main stimulation treatment.

The ISIP data cannot be used to estimate the minimum horizontal stress from large volume hydraulic fracture tests (Nolte, 1988). In this study the pressure versus square-root-of-time method is used to determine the fracture closure pressure from the pressure decline curve after shut-in and estimate the minimum horizontal stress following procedures described by Nolte (1988). Figure 2 shows an example of the pressure/time record of a hydraulic fracture treatment in a well at the Ekofisk Field from breakdown through shut-in at the completion of the fracture treatment's first phase. A plot of pressure versus square root of time of the shut-in data used to estimate the fracture closure pressure is shown in Figure 3.

There are many processes that affect the fracture closure pressure, particularly for larger fracture treatments. These effects include leakoff of fluid into the formation, in situ heterogeneities, partial fracture closure, fracture growth after shut-in, and curvature of the fracture. The error for estimating the minimum horizontal stress generally increases with the size of the fracture treatment. It is estimated that the error associated with determining the minimum horizontal stress from closure pressure data of pressure decline curves of large volume hydraulic fractures is about 0.5 to 3 MPa.

Fracture closure pressure data from large volume hydraulic fracture treatments were used to estimate the pore pressure and production-induced changes in pore pressure on minimum horizontal stress in the chalk reservoirs at the Valhall, Eldfisk, and Ekofisk Fields in the central graben of the Norwegian sector of the North Sea. Phillips Petroleum provide pressure/time records and fracture closure pressure data from the Ekofisk and Eldfisk fields and Amoco provided data from the Valhall Field. Fracture closure pressure data from large volume hydraulic fractures presented by Salz (1977) from sandstone reservoirs in the Vicksburg Formation in the McAllen Ranch Field, Texas were also used in this study.

2b. Leak-Off Test Method

Leak-off tests are commonly used by the petroleum industry to test casing integrity and can also be used to estimate the minimum horizontal stress below the casing shoe (Kunze and Steiger, 1992). The test involves drilling out the casing shoe, pulling the bit into the shoe, closing the annulus, and pumping drilling fluid into the well until formation breakdown is achieved. The standard leak-off test involves one cycle of pump-in (to create a microfracture) followed by a shut-in period (to observe fracture closure). An extended leak-off test is very similar to a conventional leak-off test except multiple cycles are used, a longer shut-in period is required, and data collection procedures/methods are more precise. The primary objective of an extended leak-off test is determine the minimum horizontal stress during the drilling operations.

Figure 4 shows an example of a pressure-time plot of an extend leak-off test. Drilling fluid is pumped into the wellbore at a constant rate until the pressure increase slows and breakdown of the formation occurs. Assuming that a fracture has been opened and propagated after breakdown, the following occurs when the pump is stopped and the well is shut-in. Initially there is a rapid decrease of the observed pressure. This is due to friction pressure loss, initial spurt loss on the fracture face and other dynamic effects. After the this initial rapid decline (instantaneous-shut-in-pressure) the pressure declines more slowly. At some point, the pressure declines to the level of the minimum horizontal stress and the fracture closes (fracture closure pressure). From this point on the leakoff is to the borehole.

Leak-off and extended leak-off test data from Phillips Petroleum and Norsk Hydro were used to estimate minimum horizontal stress in the overburden rock above the Ekofisk and Oseberg reservoirs. The procedure for the Ekofisk tests are based on the work by Kunze and Steiger (1992). The procedure is as follows:

1. Test casing to hydrostatic stress prior to drilling out shoe track. Drill out cement and three meters of new formation.
2. Rig up surface transducer to choke manifold for annular measurements.
3. Circulate drilling fluid until mud weight in/out is balanced.
4. Pull drill bit three meters into casing, hang off drill string.
5. If wireline downhole gage is used, rig up a pump-in sub, wireline blowout preventer, and pressure lubricator with downhole gage assembly.
6. Connect surface transducer to pump-in sub for drill pipe pressure measurements.
7. Run downhole gage to top of bit or baffle plate on a wireline, pull up seven meters and hang off.
8. Shut in annular blowout preventer.
9. Start pumping mud in order to create a fracture in the openhole section. Record pressure readings for every cumulative 0.04 m^3/min pumped.
10. When the breakdown occurs the pressure rise will show a change in the rate of increase. Look for a clear plateau in the pump-in pressure profile.

Continue pumping so that 5-8 pressure points are taken at the same pressure.

11. Stop pumping. Initially there is a rapid decrease in the observed surface pressure (due to the fiction pressure loss and other dynamic effects). After that the fluid is being leaked off into the fracture face and the borehole at lower rate and the pressure declines more slowly as the fracture closure occurs.

12. To obtain an accurate measure of the fracture closure pressure the well should be shut-in and pressure decline monitored for at least 30 minutes.

13. For extended leak-off tests steps 9-13 should be repeated for three cycles.

An example of the bottomhole pressure/time records for an extended leak-off test is shown in Figure 5. The test was conducted in the Ekofisk 2/4 A-11B well in overburden rock at the 13-3/8" shoe. The estimate leakoff point is at 1524.3 m, which is halfway between the casing shoe depth and the openhole depth. The test consisted of three breakdown and shut-in cycles. The minimum horizontal stress was determined from the pressure decline curve during shut-in using the pressure versus square-root-of-time method (Nolte, 1988). Figure 6 a, c, and e show each of the three leakoff test cycles separately and Figure 6 b, d, and f are the interpretation of each of the cycles to estimate the minimum horizontal stress. The fracture closure stresses and estimated values of the minimum horizontal stress were 30.5, 30.3 and 30.1 MPa for cycles 1-3, respectively. The average value of the three cycles is 30.3 MPa.

Leak-off and extended leak-off tests were used to estimate the minimum horizontal stress in overburden rock (shales and mudstones) in the Ekofisk and Oseberg Fields, North Sea. Pressure/time records and leak-off test data from the Ekofisk Field were provided by Phillips Petroleum and Norsk Hydro provided data from the Oseberg Field. In this study an estimate of the fracture closure pressure was estimated using the bottomhole pressure versus the square-root-of-time method (Nolte, 1988). This is a standard procedure used by the petroleum industry and is identical to the procedure used to estimate closure pressure in small and large volume hydraulic fracture tests.

3. IN SITU STRESS MEASUREMENTS

3a. Valhall Field, North Sea

The Valhall Field is an overpressured, undersaturated Upper Cretaceous chalk reservoir located 290 km offshore in the central graben of the North Sea at the southern tip of the Norwegian sector (Figure 7). The field was discovered in 1975, and field development began in 1981 (Kennedy, 1985). The reservoir is at a depth of about 2,400 m subsea and consists of two oil bearing formations: the Tor and Hod. About two-thirds of the oil and the majority of the production are in the Tor formation, which is a soft chalk characterized by very high porosity (up to 50%) and very high oil saturations (90% or

greater). Although the chalk has high porosity the matrix permeability is less than 1×10^{-15} m^2.

Hydraulic fracture stimulations are routinely conducted in the field to improve oil recovery. Minimum horizontal stress magnitudes have been estimated from closure pressure data from the first phase of these stimulations in the Tor formation. A total of 20 measurements were made in nine wells. Ten of the measurements were made at the start of production in the field and represent initial stress and pore pressure conditions in the reservoir. The same zones in the nine wells were later hydraulically fractured a second time, to improve production after the reservoir pressure was drawn down. These ten measurements provide information on the effect of pore pressure drawdown on horizontal stress. Pore pressure was determined from well tests before the stimulation treatments. Table 1 summarizes all of the in situ stress and corresponding pore pressure data from the Valhall Field.

The total vertical stress, total minimum horizontal stress, and pore pressure as a function of depth for the initial reservoir conditions before production are shown in Figure 8. The total vertical stress was calculated from the weight of the overlying rock using an integrated formation density log. The total vertical and horizontal stresses and pore pressure increase linearly with depth. The total vertical stress gradient is 20.3 kPa/m, the total horizontal stress gradient is 17.6 kPa/m, and the pore pressure gradient is 16.1 kPa/m.

The effective stress state can also be determined from this data. Following Rice and Cleary (1976) effective stress is defined by:

$$\sigma = S - \alpha P$$

where σ is the effective stress, S is the total stress, α is a poroelastic parameter, and P is the pore pressure. For this study α is assumed to equal unity. Figure 9 shows the relationship between the minimum effective horizontal stress and effective vertical stress before production. A linear regression analysis of the data shows that at initial reservoir conditions the ratio of change in minimum effective horizontal stress to change in effective vertical stress with increasing depth and pore pressure is 0.68. The correlation coefficient of this linear fit is 0.995.

The effect of pore pressure drawdown on horizontal stress is shown in Figure 10. With a decrease in pore pressure the total minimum horizontal stress shows a significant decrease. A linear regression analysis of the data shows that the change in total minimum horizontal stress to net change in pore pressure as a result of production is 0.75. The correlation coefficient of this linear fit is 0.956.

Measurements of the total minimum horizontal stress as a function of pore pressure drawdown can be used to provide an understanding of the boundary conditions on the reservoir and the stress path followed by reservoir rock during the production

history. With pore pressure draw down the effective stresses in the reservoir increase, but at different rates. Figure 11 shows the relationship between effective vertical stress and minimum effective horizontal stress before and after production. A linear regression analysis of the data shows that the ratio of change in effective minimum horizontal stress to change in effective vertical stress is 0.28. Thus, with pore pressure drawdown the minimum effective horizontal stress has increased at a much slower rate than the effective vertical stress. Moreover, for the Valhall reservoir the stress path followed by the chalk formations during production and pore pressure depletion is much lower than the stress state that developed over time by geologic processes.

3b. Eldfisk Field, North Sea

The Eldfisk Field is the second largest of nine chalk reservoirs in the southern part of the Norwegian sector of the North Sea (Figure 7.) It is an elliptical dome, elongate in a north-south direction. Oil production is from two intervals: the Upper Cretaceous Tor and Hod formations (Kennedy, 1985). Both formations are high-porosity, naturally-fractured chalk. The top of the reservoir is at a depth of 2,800 m. The high porosity chalk in this reservoir has low permeability and hydraulic fracture stimulations are conducted in each well to improve oil productivity. Closure pressure data from 14 of these stimulation treatments in the Tor formation have been used to estimate the total minimum horizontal stress. All of these hydraulic fractures were conducted after production began and knowledge of the initial horizontal stress state is not known. Pore pressure at the time of discovery in 1973 was about 45 MPa. Pore pressure has been monitored in the reservoir as it has been produced. Well tests before each of the stimulation treatments were used to measure the pore pressure. Table 2 summarizes all of the available in situ stress and corresponding pore pressure data from the Eldfisk Field.

The total minimum horizontal stress decreases as the reservoir pore pressure declines (Figure 12). A linear regression analysis of the data shows that the change in minimum horizontal stress is about 86 percent of the net change in pore pressure. The correlation coefficient of this linear fit is 0.895. Figure 13 is a normalized plot of the same data as a function depth and shows the linear relationship between the total minimum horizontal stress gradient and pore pressure gradient. The slope of the best fit line is 0.84. The correlation coefficient of the linear fit is 0.924.

Figure 14 shows the relationship between the effective vertical stress and minimum effective horizontal stress as the reservoir pore pressure has been drawn down. Using a linear regression analysis the ratio of change in effective horizontal stress to change in effective vertical stress is 0.15. Hence, with pore pressure drawdown the minimum effective horizontal stress has increased at a much slower rate than the effective vertical stress.

3c.   Ekofisk Field, North Sea

The Ekofisk field is the largest of nine chalk reservoirs in the southern part of the Norwegian sector of the North Sea. It is an elliptical dome, elongate in a north-south direction. The reservoir consists of two naturally-fractured chalk formations separated by a relatively impermeable layer of argillaceous, siliceous, and cherty chalk. Porosity ranges from 5-51%, but averages 32% in the Ekofisk formation and 30% in the Tor formation (Feazel et al, 1990). The high porosity chalk has low matrix permeability and hydraulic fracture stimulations are conducted in each well to improve oil productivity. Closure pressure data from 32 hydraulic fracture treatments in the Ekofisk and Tor formations have been used to estimate the total minimum horizontal stress. All of these hydraulic fractures were conducted after production began and knowledge of the initial horizontal stress state is not known. Pore pressure at the time of discovery in 1969 was about 48.5 MPa. Pore pressure has been monitored in the reservoir as it has been produced. Well tests before each of the stimulation treatments were used to measure the pore pressure. Table 3 summarizes all of the available in situ stress measurements and corresponding pore pressure data from chalk reservoirs in the Ekofisk Field.

In the Ekofisk chalk reservoirs the total minimum horizontal stress decreases as the pore pressure declines with production (Figure 15). A linear regression analysis of the data shows that the change in minimum horizontal stress is about 80 percent of the net change in pore pressure. The correlation coefficient of this linear fit is 0.891. Figure 16 is a normalized plot of the same data as a function depth and shows the linear relationship between the total minimum horizontal stress gradient and pore pressure gradient. The slope of the best fit line is 0.78. The correlation coefficient of the linear fit is 0.906.

Figure 17 shows the relationship between the effective vertical stress and minimum effective horizontal stress as the reservoir pore pressure has been drawn down. Using a linear regression analysis the ratio of change in effective horizontal stress to change in effective vertical stress is 0.22. The minimum effective horizontal stress has increased at a much slower rate than the effective vertical stress with pore pressure drawdown.

For the three North Sea chalk fields the stress paths followed by the reservoir rock during production and pore pressure drawdown are similar. The stress paths are 0.15 for Eldfisk, 0.22 for Ekofisk , and 0.28 for Valhall.

Horizontal stress measurements have also been obtained from the overburden rock above the Ekofisk reservoir. The Ekofisk overburden is composed of mudstone and shales. Twelve extended leak-off tests were used to estimate the total minimum horizontal stress. Tests were conducted at a depth from 520 to 2884 meters. Table 4 summarizes all of the available in situ stress data and corresponding pore pressure data for the Ekofisk overburden. Quality of the pore pressure data is not good. Pore pressure is an estimate based on drilling mud logs provided by Phillips Petroleum.

Total vertical stress, total minimum horizontal stress, and pore pressure as a function of depth in the Ekofisk overburden rock is shown in Figure 18. The total vertical stress was calculated from the weight of the overlying rock using an integrated formation density log. The horizontal and vertical stresses are nearly equal. The average minimum horizontal stress gradient is 18.5 kPa/m compared to an average vertical stress gradient of 20.1 kPa/m.

Figure 19 shows the relationship between effective vertical stress and minimum effective horizontal stress in the overburden. Using a linear regression analysis the ratio of change in effective horizontal stress to change in effective vertical stress is 0.95. Effective horizontal and vertical stresses are essentially equal in the overburden. Stress measurements in the Ekofisk field clearly show that the stress state in the overburden rock is significantly different from the stress state in reservoir chalks.

3d. Oseberg Field, North Sea

The Oseberg Field is located in the Viking graben in the Norwegian sector of the North Sea approximately 140 km northwest of Bergen, Norway. The Oseberg Field is comprised of three large fault blocks inclined at angles of six to ten degrees to the northeast. Hydrocarbons are produced from two Jurassic age sandstone reservoirs in these fault blocks at depths ranging from 2,600 to 2,950 m (Johnsen, 1988). Production from the field began in 1989 and pore pressure is being maintained in the field by gas and water injection. The overburden rock overlying the reservoirs are Tertiary and Cretaceous age shales and mudstones.

Leak-off tests have been used to estimate the minimum horizontal stress in the Oseberg overburden rock. A total of 73 tests in 36 wells were analyzed at depths from 471 m to 2,900 m. Table 5 summarizes all of the available in situ stress and pore pressure data from the overburden rock in the Oseberg Field. The pore pressure data used for the Oseberg overburden is an estimate based on drilling mud logs provided Norsk Hydro.

Total vertical stress, total minimum horizontal stress, and pore pressure as a function of depth in the Oseberg overburden rock is shown in Figure 20. The total vertical stress was calculated from the weight of the overlying rock using an integrated formation density log. The vertical stress gradient is nonlinear between 400 m and 900 m with an average gradient of 19.7 kPa/m. Below 900 m the vertical stress is linear with a gradient of 20.1 kPa/m. The total minimum horizontal stress is greater than the vertical stress near the surface and becomes less than the vertical stress at depth. The pore pressure is normally pressured at depths down to about 1,500 m, becomes overpressured between approximately 1,500 and 2,500 m, and returns to a normal pressure gradient below about 2,500 m.

Figure 21 shows the relationship between pore pressure and total minimum horizontal stress for Oseberg overburden rock as a function of depth. The relationship between effective vertical stress and minimum effective horizontal stress is shown in

Figure 22. Using a linear regression analysis the ratio of change in effective horizontal stress to change in effective vertical stress is 0.53.

The lithology of the overburden formations at the Oseberg and Ekofisk Fields are very similar. However, the total and effective horizontal stresses are very different. The ratio of change in effective horizontal stress to change in effective vertical stress with increasing depth is 0.95 at the Ekofisk Field and a much lower 0.53 at the Oseberg Field. Local geologic conditions must be the cause of this difference.

3e.   McAllen Ranch Field, Texas

Salz (1977) presented hydraulic fracture stress data and pore pressure measurements from reservoir pressure buildup tests in sandstones of the Vicksburg formation in the McAllen Ranch Field, Texas. This work was one of the first studies to clearly show that the total minimum horizontal stress is dependent on the pore pressure. Hydraulic fractures were completed in underpressured and overpressured sandstone intervals from approximately 3,100 to 3,800 m. Some of the sandstones were later hydraulically fractured a second time to improve oil productivity after the reservoir pressure had been drawn down. Table 6 is a summary of 20 stress measurements and corresponding pore pressure data presented by Salz (1977).

For initial reservoir conditions before production the total minimum horizontal stress showed a decrease with decreasing pore pressure for the different sandstone reservoirs (Figure 23). A linear regression analysis of the data shows that the change in minimum horizontal stress is about 57 percent of the net change in pore pressure. The correlation coefficient of this linear fit is 0.889. Figure 24 is a normalized plot of the same data as a function depth and shows the linear relationship between the total minimum horizontal stress gradient and pore pressure gradient. The slope of the best fit line is 0.54. The correlation coefficient of the linear fit is 0.942.

Figure 25 shows the linear relationship between the minimum effective horizontal stress and effective vertical stress before production. At initial reservoir conditions the change in minimum effective horizontal stress was equal to about 48 percent of the net change in effective vertical stress.

Figure 26 is a plot of pore pressure versus total minimum horizontal stress in six sandstone reservoirs before and after production. A linear regression analysis of the data shows that the decrease in total minimum horizontal stress is about 48 percent of the net change in pore pressure. The correlation coefficient of this linear fit is 0.980. Figure 27 is a normalized plot of this data as a function of depth and shows the linear relationship between the total minimum horizontal stress gradient and pore pressure gradient. The slope of the best fit line is 0.47. The correlation coefficient of the linear fit is 0.982.

The relationship between effective vertical stress and effective minimum horizontal stress in the same sandstone reservoirs before and after production is shown in Figure 28.

Using a linear regression analysis the ratio of change in effective horizontal stress to change in effective vertical stress is 0.53 as a result of production. This effective stress relationship is essentially the same for production-induced or geologically-induced (before production) changes in pore pressure.

3f.   Rulison Field, Colorado

Warpinski and Teufel (1989) presented hydraulic fracture stress measurements from a series of sandstones in the Mesaverde formation at the Rulison Field, Colorado. The Mesaverde sandstones are isolated tight-gas reservoirs of fluvial and deltaic origins. Pore pressure in these reservoirs are overpressured and vary with depth. Table 7 is a summary of 16 hydraulic fracture stress measurements and corresponding pore pressure data from five zones in the MWX-2 well before production.

Total vertical stress, total minimum horizontal stress, and pore pressure as a function of depth for the Mesaverde sandstones are shown in Figure 29. The total minimum horizontal stress increases with depth, but pore pressure shows significant variation with depth. Figure 30 is a plot of pore pressure versus total minimum horizontal stress and shows considerable scatter. However, the plot of effective vertical stress versus effective horizontal stress shows a much tighter fit (Figure 31). Using a linear regression analysis the ratio of change in minimum effective horizontal stress to change in effective vertical stress is 0.65.

4.   DISCUSSION

Reservoirs are dynamic systems that are constantly changing during their geologic evolution and later, during their production history. Primary hydrocarbon production of a reservoir will reduce the pore pressure, increase the effective stresses, and change the three dimensional effective-stress field. Measurements of the total minimum horizontal stress as a function of pore pressure drawdown can be used to provide an understanding of the boundary conditions on the reservoir and the stress path followed by reservoir rock during the production history.

In situ stress measurements made during pore pressure drawdown of three North Sea chalk reservoirs clearly demonstrate that the stress paths followed by reservoir rock of these adjacent fields during production and pore pressure depletion are similar. The stress paths are 0.15 for Eldfisk, 0.22 for Ekofisk, and 0.28 for Valhall. These stress paths are significantly less than either a constant total stress boundary condition (hydrostatic or isotropic loading and the stress path equals 1.0) or a uniaxial strain boundary condition (i.e., no lateral displacement of the reservoir boundaries and the stress path equal to 0.4 to 0.6, as determined by uniaxial strain tests on reservoir chalk (Johnson et al., 1989)).

The in situ stress data of the Vicksburg sandstones in the McAllen Ranch Field from Salz (1977) also do not agree with either the total stress or uniaxial strain boundary

conditions. Production-induced changes in effective stresses in the Vicksburg sandstones indicate a stress path of 0.53, which is less than the 1.0 for the total stress boundary condition, but greater than the predicted 0.25 - 0.33 stress path for an elastic uniaxial-strain boundary condition (based on elastic properties of Vicksburg sandstone in Salz, 1977). The measured stress path 0.65 in the Mesaverde sandstones in the Rulison Field is also greater than the calculated elastic uniaxial-strain stress path of 0.18 - 0.28 (based on elastic properties of Mesaverde sandstones in Warpinski, et al., 1985). .

The significance of stress path is that shear stresses increase more rapidly with pore pressure drawdown for reservoirs following low stress paths than for reservoirs following high stress paths. The measured stress paths of the chalk and sandstone reservoirs presented in this study are always less than the total stress boundary condition (isotropic loading) and are either greater or less than the stress path predicted by the uniaxial strain boundary condition. Clearly, these two boundary-condition models, that are commonly used by the petroleum industry to calculate changes in effective stresses in a reservoir and measure reservoir properties in the laboratory, are inaccurate and can be misleading if applied to reservoir management problems. Other models have been proposed to calculate in situ stresses, but they depend on a complex history of properties and loading conditions (Voight, 1974; Rosepiler, 1979; Prats, 1981; Warpinski, 1989). Application of these models is limited because of the large uncertainty in mechanical properties of large rock masses and loading conditions in the subsurface.

Reservoir stress path is probably a function of several different factors. These factors include boundary conditions on the reservoir, size and geometry of the reservoir, reservoir depth, poroelastic deformation behavior of reservoir rock and bounding formations, and other parameters. At present, the only way to determine the stress path is to measure the in situ horizontal stresses at two or more different drawdown pressures.

5.   CONCLUSIONS

A compendium of in situ stress data from six oil and gas fields has been organized to show the effects of pore pressure and production-induced changes in pore pressure on the minimum horizontal in situ stress. The in situ stress data and corresponding pore pressure data were obtained from field records of the operating companies and published reports. Horizontal stress was determined from closure pressure data of hydraulic fractures and leak-off tests. The stress measurements clearly demonstrate that the total minimum-horizontal stress is dependent on pore pressure. A decrease in pore pressure either by geologic processes or production of a reservoir will result in a decrease in the total minimum-horizontal stress. The magnitude of changes in stress state with net changes in pore pressure is dependent on local field conditions and cannot be accurately predicted by the uniaxial strain model that is commonly used by the petroleum industry.

6.   ACKNOWLEDGMENTS

7.   REFERENCES

Bell, J.S. and D.T. Gough, 1982, "The Use of Borehole Breakouts in the Study of Crustal Stress," in Proc. of Hydraulic Fracturing Stress Measurements, U.S. Geologic Survey Open File Report 82-1075, Denver, CO.

Feazel, C.T., I.A. Knight, and L.J. Pekot, 1990, "Ekofisk Field, Norwegian Sector, North Sea," in Am. Assoc. Petro. Geol. Atlas of Petroleum Geology, 424-456.

Hubbert, M.K. and G.D. Willis, 1957, "Mechanics of Hydraulic Fracturing," Trans. AIME, 210, 153-166.

Johnsen, R.J., 1988, "Jurassic Reservoirs; Field Examples from the Oseberg and Troll Fields, Horda Platform Area," Norsk Hydro Report.

Johnson, J.P., D.W. Rhett, and W.T. Siemers, 1989, "Rock Mechanics of the Ekofisk Reservoir in the Evaluation of Subsidence," J. Petro. Tech., 41, 717-722.

Kehle, R.O., 1961, "Determination of Tectonic Stresses through Analysis Hydraulic Well Fracturing," J. Geopys. Res, 69, 259-278.

Kennedy, W.J., 1985, "Sedimentology of the Late Cretaceous and Early Palaeocene Chalk Group, North Sea Central Graben," in North Sea Chalk Symp. Book 1, 1-35.

Kunze, K.R. and R.P. Steiger, 1992, "Accurate In Situ Stress Measurements During Drilling Operations," paper SPE 24593 presented at the 1992 SPE Annual Technical Conference, Washington, D.C., Oct. 3-6.

Nolte, K.G., 1988, Principles for Fracture Design Based on Pressure Analysis," SPE Production Engineering, 3, 31-42.

Prats, M., 1981, "Effect of Burial History on the Subsurface Horizontal Stresses of Formations Having Different Material Properties," SPEJ, 28, 658-62.

Ren, N.K. and J.C. Roegiers, 1983, "Differential Strain Curve Analysis - A New Method for Determining the Preexisting In Situ Stress State from Rock Core Measurements," Proc. ISRM Congress, Melbourne, F117-27.

Ren, N.K. and P.J. Hudson, 1985, "Predicting In Situ Stress State Using Differential Wave Velocity Analysis," Proc. 26th Symp. on Rock Mechanics, Rapid City, SD, 1235-46.

Rice, J. and M. Cleary, 1976, "Some Basic Stress Diffusion Solutions for Fluid-Saturated Elastic Porous Media with Compressible Constituents, Rev. Geophys. and Space Phys., 14, 227-241.

Rosepiler, M.J., 1979, "Determination of Principal Stresses and Confinement of Hydraulic Fractures in Cotton Valley," paper SPE 8405 presented at the 1979 SPE Annual Technical Conference, Las Vegas, Sept. 23-26.

Salz, L.B., 1977, "Relationship Between Fracture Propagation Pressure and Pore Pressure," paper SPE 6870 presented at 1977 SPE Annual SPE Conference, Denver, CO, Oct. 9-12.

Teufel, L.W., 1983, "Determination of In Situ Stress from Anelastic Strain Recovery Measurements of Oriented Core," paper SPE 11649 presented at the 1983 SPE/DOE Symp. on Low Permeability, Denver, CO, March 14-16.

Voight, B., 1974, "Stress History and Rock Stress," Third Intl. Congress of Soc. Rock Mechanics, 2, Part A, 580-82.

Warpinski, N.R, P.T Branagan, R. Wilmer, 1985, "In Situ Stress Measurements at DOE's Multiwell Experiement Site, Mesaverde Group, Rifle, Colorado, J. Petro. Tech., 37, 527-36.

Warpinski, N.R., 1989, "Elastic and Viscoelastic Calculations of Stresses in Sedimentary Basins," SPE Formation Evaluation, 3, 522-530.

Warpinski, N.R. and L.W. Teufel, 1989, "In Situ Stress Measurements in Low-Permeability, Non-Marine Rocks," J. Petro. Tech., 41, 405-414.

EXTERNAL DISTRIBUTION:

Exxon Company USA (2)
P. O. Box 2180
800 Bell
Houston, TX 77252
    Jeffery Davis
    Mike Lukk

ARCO Alaska (3)
P. O. Box 100360
Anchorage, AK 99510
    Don Chancey
    Monte Mabry
    Charles Landmesser

Robert Hunter (1)
BP Exploration
P. O. Box 196612
Anchorage, AK 99519

Bob Lemmon (10)
U. S. Department of Energy
P. O. Box 1398
Bartlesville, OK 94005

Cathy Hanks (5)
School of Earth Sciences
La Trobe University
Bundoora, Victoria 3083
AUSTRALIA

Andrea Krumhardt (1)
Dept. of Geology
University of Alaska
Fairbanks, AK 99775

INTERNAL DISTRIBUTION:

MS0751	S. R. Brown (6117) (1)
MS0751	J. T. Fredrich (6117) (1)
MS0751	D. J. Holcomb (6117) (1)
MS0751	J. C. Lorenz (6117) (5)
MS0751	R. M. O'Connor (6117) (1)
MS0751	W. A. Olsson (6117) (1)
MS0751	D. S. Preece (6117) (1)
MS0751	W. R. Wawersik (6117) (1)
MS0751	D. H. Zeuch (6112) (1)
MS0751	File (6117) (5)
MS0702	L. W. Teufel (6200) (5)
MS0702	File (6200) (1)
MS0100	Document Processing (7613-2) for DOE/OSTI (2)
MS9018	Central Technical Files (8523-2) (1)
MS0619	Print Media (12615) (1)
MS0899	Technical Library (4414) (5)

Table 1. Summary of in situ stress data from chalk reservoirs in the Valhall Field, North Sea.								
		Total	Total Minimum		Effective	Effective	Total	Pore
		Vertical	Horizontal	Pore	Vertical	Horizontal	Horizontal	Pressure
WELL	Depth	Stress	Stress	Pressure	Stress	Stress	Stress Gradient	Gradient
	(M)	(MPa)	(MPa)	(MPa)	(MPa)	(MPa)	(KPa/M)	(KPa/M)
A-11A	2,522	51.23	47.82	44.74	6.50	3.08	18.96	17.74
A-11A	2,522	51.23	45.76	41.97	9.26	3.78	18.15	16.64
A-16A	2,491	50.60	46.92	44.53	6.08	2.39	18.84	17.88
A-16A	2,491	50.60	41.29	36.19	14.41	5.09	16.58	14.53
A-3A	2,479	50.36	46.58	44.45	5.91	2.13	18.79	17.93
A-3A	2,479	50.36	40.18	35.44	14.92	4.75	16.21	14.30
A-13B	2,478	50.35	46.56	44.44	5.91	2.12	18.79	17.93
A-13B	2,478	50.35	40.32	35.09	15.26	5.23	16.27	14.16
A-4	2,473	50.24	46.40	44.41	5.83	1.99	18.77	17.96
A-4	2,473	50.24	38.37	34.11	16.13	4.27	15.52	13.80
A-7	2,453	49.83	45.82	44.27	5.56	1.55	18.68	18.05
A-7	2,453	49.83	42.05	38.82	11.01	3.23	17.15	15.83
A-24	2,583	52.48	49.59	45.15	7.33	4.44	19.20	17.48
A-24	2,583	52.48	45.96	39.91	12.57	6.06	17.79	15.45
A-13B	2,563	52.07	49.02	45.02	7.05	4.00	19.13	17.57
A-13B	2,563	52.07	44.24	38.95	13.13	5.30	17.26	15.20
A-1	2,482	50.43	46.67	44.47	5.96	2.20	18.81	17.92
A-1	2,482	50.43	35.57	30.62	19.81	4.95	14.33	12.34
A-1	2,548	51.76	48.57	44.91	6.85	3.65	19.06	17.63
A-1	2,548	51.76	37.78	29.24	22.52	8.53	14.83	11.48

Table 2. Summary of in situ stress data from chalk reservoirs in the Eldfisk, North Sea.								
		Total	Total Minimum		Effective	Effective	Total	Pore
		Vertical	Horizontal	Pore	Vertical	Horizontal	Horizontal	Pressure
WELL	Depth	Stress	Stress	Pressure	Stress	Stress	Stress Gradient	Gradient
	(M)	(MPa)	(MPa)	(MPa)	(MPa)	(MPa)	(KPa/M)	(KPa/M)
2/7-B6	2,925	58.76	42.80	33.51	25.25	9.29	14.63	11.46
2/7-B8	2,986	59.99	50.51	41.97	18.01	8.53	16.92	14.06
2/7-B3	3,001	60.29	43.56	37.23	23.06	6.33	14.51	12.40
2/7-B1	2,938	59.02	40.25	34.93	24.09	5.32	13.70	11.89
2/7-B1	2,909	58.44	43.62	34.47	23.97	9.15	15.00	11.85
2/7-B2	3,032	60.91	49.34	39.04	21.87	10.30	16.27	12.88
2/7-B10	2,999	60.25	44.59	39.15	21.10	5.44	14.87	13.06
2/7-B4	3,009	60.45	46.65	39.01	21.43	7.64	15.51	12.97
2/7-A8	3,011	60.50	34.92	26.42	34.07	8.50	11.60	8.78
2/7-A9	2,951	59.30	38.05	27.62	31.68	10.43	12.89	9.36
2/7-A1	3,001	60.29	39.77	31.34	28.95	8.44	13.25	10.44
2/7-A2	2,860	57.45	36.76	26.39	31.06	10.37	12.85	9.23
2/7-A4	2,998	60.23	43.76	33.82	26.41	9.94	14.60	11.28
2/7-A6	2,964	59.55	36.81	27.76	31.80	9.06	12.42	9.36

Table 3. Summary of in situ stress data from chalk reservoirs in the Ekofisk Field, North Sea								
		Total	Total Minimum		Effective	Effective	Total	Pore
		Vertical	Horizontal	Pore	Vertical	Horizontal	Horizontal	Pressure
WELL	Depth	Stress	Stress	Pressure	Stress	Stress	Stress Gradient	Gradient
	(M)	(MPa)	(MPa)	(MPa)	(MPa)	(MPa)	(KPa/M)	(KPa/M)
2/4-A5	3,331	63.20	53.10	45.50	17.70	7.60	15.94	13.66
2/4-A9	3,170	63.80	50.30	40.60	23.20	9.70	15.87	12.81
2/4-A13	3,128	63.00	46.90	38.20	24.80	8.70	14.99	12.21
2/4-B6	3,144	63.30	37.20	26.80	36.50	10.40	11.83	8.52
2/4-B15	3,189	64.20	41.40	34.00	30.20	7.40	12.98	10.66
2/4-B23	3,126	63.00	38.60	25.50	37.50	13.10	12.35	8.16
2/4-C6	3,152	63.50	35.80	24.10	39.40	11.70	11.36	7.65
2/4-C7	3,128	63.00	33.80	25.50	37.50	8.30	10.81	8.15
2/4-C15	3,109	62.60	42.90	33.80	28.80	9.10	13.80	10.87
2/4-K1	3,158	63.60	34.30	26.40	37.20	7.90	10.86	8.36
2/4-K4	3,132	63.10	34.50	26.20	36.90	8.30	11.02	8.37
2/4-K5	3,115	62.70	38.60	28.90	33.80	9.70	12.39	9.28
2/4-K10	3,177	64.00	39.00	27.40	36.60	11.60	12.28	8.62
2/4-K11	3,175	63.90	38.60	26.70	37.20	11.90	12.16	8.41
2/4-K13	3,143	63.30	35.80	27.20	36.10	8.60	11.39	8.65
2/4-K20	3,200	64.50	37.20	28.80	35.70	8.40	11.62	9.00
2/4-K17	3,139	63.20	40.00	31.20	32.00	8.80	12.74	9.94
2/4-K21	3,123	62.90	45.20	28.80	34.10	16.40	14.47	9.22
2/4-K23	3,196	64.40	46.60	35.20	29.20	11.40	14.58	11.01
2/4-K24	3,210	64.70	39.10	25.40	39.30	13.70	12.18	7.91
2/4-K27	3,183	64.10	40.30	25.50	38.60	14.80	12.66	8.01
2/4-K29	3,158	63.60	42.00	27.40	36.20	14.60	13.30	8.68
2/4-K30	3,257	65.60	43.50	28.60	37.00	14.90	13.36	8.78
2/4-K8	3,200	64.50	52.40	41.10	23.40	11.30	16.37	12.84
2/4-A20	3,216	64.80	45.80	31.70	33.10	14.10	14.24	9.86
2/4-A18	3,103	62.50	50.40	44.60	17.90	5.80	16.24	14.37
2/4-B20	3,109	62.60	40.00	32.50	30.10	7.50	12.87	10.45
2/4-B14	3,145	63.30	35.00	26.20	37.10	8.80	11.13	8.33
2/4-B10	3,115	62.70	34.80	26.20	36.50	8.60	11.17	8.41
2/4-C12	3,165	63.70	34.00	26.60	37.10	7.40	10.74	8.41
2/4-C17	3,078	62.00	47.60	42.20	19.80	5.40	15.46	13.71
2/4-K19	3,103	62.50	43.50	36.90	25.60	6.60	14.02	11.89

Table 4. Summary of in situ stress data from overburden rock in the Ekofisk Field, North Sea								
		Total	Total Minimum		Effective	Effective	Total	Pore
		Vertical	Horizontal	Pore	Vertical	Horizontal	Horizontal	Pressure
WELL	Depth	Stress	Stress	Pressure	Stress	Stress	Stress Gradient	Gradient
	(M)	(MPa)	(MPa)	(MPa)	(MPa)	(MPa)	(KPa/M)	(KPa/M)
2/4A-02	1,527	29.81	27.30	20.50	9.31	6.80	17.88	13.15
2/4A-11E	520	9.18	7.90	5.25	3.93	2.65	15.19	10.10
2/4A-11E	1,524	29.75	30.30	20.03	9.72	9.47	19.88	13.15
2/4A-11E	1,761	34.60	30.30	26.60	8.00	3.70	17.21	15.11
2/4A-15C	1,548	30.37	29.50	20.80	9.57	8.70	19.06	13.44
2/4A-24E	1,498	29.39	30.00	18.08	11.32	11.22	20.03	12.07
2/4C-08B	1,328	25.01	26.00	13.68	11.33	12.32	19.58	10.30
2/4C-08B	2,884	58.56	53.80	44.70	13.86	9.10	18.65	15.50
2/4C-09A	1,318	24.77	25.30	13.58	11.19	11.72	19.20	10.30
2/4C-09A	2,884	58.57	56.30	44.71	13.86	11.59	19.52	15.50
2/4K-06	1,500	28.25	26.00	18.25	10.01	7.75	17.33	12.16
2/7B-08A	1,496	28.18	27.10	18.20	9.98	8.90	18.11	12.16

WELL	Depth (M)	Total Vertical Stress (MPa)	Total Minimum Horizontal Stress (MPa)	Pore Pressure (MPa)	Effective Vertical Stress (MPa)	Effective Horizontal Stress (MPa)	Total Horizontal Stress Gradient (KPa/M)	Pore Pressure Gradient (KPa/M)
30/9-14	471	6.70	8.63	4.18	2.52	3.87	18.32	8.87
30/6-13	600	9.06	8.22	5.47	3.59	2.16	13.69	9.12
306/14	601	9.08	10.21	5.48	3.60	4.14	16.98	9.12
306/19	602	9.09	8.27	5.49	3.60	2.19	13.74	9.12
306/20	603	9.11	10.08	5.50	3.61	3.99	16.72	9.12
30/6-C06	968	15.95	15.19	9.20	6.75	5.41	15.70	9.51
30/9-2	1,680	30.16	28.91	17.55	12.61	11.94	17.21	10.45
30/9-2	901	14.73	15.71	8.52	6.20	6.61	17.44	9.46
30/9-6	955	15.70	15.75·	9.08	6.62	6.11	16.50	9.51
30/9-7	1,057	17.73	18.13	10.09	7.64	7.45	17.15	9.55
30/9-8	1,044	17.49	16.28	9.97	7.53	5.73	15.59	9.55
30/9-13s	1,131	19.23	18.40	10.83	8.40	6.97	16.27	9.57
30/9-13s	1,017	16.97	17.03	9.68	7.29	6.76	16.75	9.52
30/9-B05A	1,109	18.78	17.55	10.62	8.16	6.78	15.83	9.57
30/9-B15	1,013	16.90	16.46	9.64	7.26	6.23	16.25	9.52
30/9-B18	1,060	17.78	16.25	10.12	7.66	5.54	15.33	9.55
309/b26	834	13.47	12.11	7.83	5.63	3.70	14.53	9.40
309/B39	1,627	29.10	26.55	16.30	12.80	10.11	16.32	10.02
309/B42	1,514	26.84	24.73	14.70	12.13	9.44	16.33	9.71
306/7	952	15.71	14.14	9.05	6.66	4.52	14.85	9.51
30/6-10	949	15.66	14.20	9.02	6.64	4.61	14.96	9.51
30/6-10st	1,788	32.45	27.06	19.91	12.54	7.77	15.13	11.13
30/6-11	951	16.86	15.24	9.04	7.82	5.63	16.02	9.51
306/14	1,648	29.54	28.14	17.22	12.32	11.49	17.08	10.45
30/6-24S	1,004	16.69	15.23	9.55	7.14	5.09	15.17	9.52
306/17R	1,593	28.29	27.13	15.52	12.77	11.04	17.03	9.74
30/6-C01	1,410	24.70	21.64	13.65	11.05	3.53	15.35	9.68
30/6-24S	1,004	16.69	15.23	9.55	7.14	5.09	15.17	9.52
30/6-C01	1,410	24.73	20.23	13.65	11.08	2.12	14.35	9.68
30/6-C04	1,168	19.89	18.47	11.21	8.69	5.41	15.81	9.59
30/6-C05	1,006	16.73	14.65	9.57	7.15	4.49	14.56	9.52
30/6-C08	1,000	16.63	15.35	9.52	7.11	5.25	15.35	9.52
30/6-C18	1,357	23.74	22.41	13.14	10.60	7.77	16.51	9.68
30/6-C21	1,132	19.24	13.23	10.83	8.40	2.69	11.69	9.57
30/6-C24	1,103	18.68	17.19	10.56	8.12	6.05	15.59	9.57
30/9-9	2,180	41.23	36.51	28.02	13.22	14.49	16.75	12.85

Table 5. Summary of in situ stress data from overburden rock in the Oseberg Field, North Sea

		Total	Total Minimum		Effective	Effective	Total	Pore
		Vertical	Horizontal	Pore	Vertical	Horizontal	Horizontal	Pressure
WELL	Depth	Stress	Stress	Pressure	Stress	Stress	Stress Gradient	Gradient
	(M)	(MPa)	(MPa)	(MPa)	(MPa)	(MPa)	(KPa/M)	(KPa/M)
306/7	2,265	43.11	38.46	29.11	14.00	9.58	16.98	12.85
30/6-10	2,138	40.10	34.04	27.37	12.73	9.51	15.92	12.80
30/6-11	2,106	39.46	34.31	27.06	12.40	9.32	16.29	12.85
30/6-C21	2,019	37.63	30.97	25.15	12.48	4.63	15.34	12.46
30/9-1	2,493	48.42	43.87	27.88	20.54	13.80	17.60	11.18
30/9-4	2,757	54.55	45.91	26.78	27.78	11.30	16.65	9.71
30/9-8	2,651	52.14	41.24	25.56	26.58	13.17	15.56	9.64
30/9-12	2,528	49.30	40.59	28.15	21.15	12.33	16.06	11.13
30/9-B18	2,493	48.42	38.25	28.37	20.05	13.07	15.34	11.38
309/B26	2,509	48.81	38.49	27.94	20.87	10.68	15.34	11.13
309/B32	2,527	49.28	38.62	28.14	21.15	13.10	15.28	11.13
309/B40	2,524	49.22	41.95	28.10	21.12	13.73	16.62	11.13
309/B46	2,531	49.36	42.92	28.18	21.18	15.62	16.96	11.13
309/B50h	2,491	48.38	38.50	28.35	20.04	11.87	15.46	11.38
306/9	2,384	45.89	41.65	29.19	16.70	11.25	17.47	12.24
306/19	2,790	55.29	51.25	27.10	28.19	12.00	18.37	9.71
30/6-22	2,778	54.99	44.99	26.98	28.02	10.39	16.19	9.71
30/6-24S	2,868	57.11	50.22	27.85	29.26	16.47	17.51	9.71
30/6-C07	2,523	49.20	42.16	28.09	21.11	14.45	16.71	11.13
30/6-C07	2,523	49.20	41.84	28.09	21.11	14.13	16.59	11.13
30/6-C09	2,527	49.28	35.98	28.14	21.15	7.48	14.24	11.13
30/9-B15	2,499	48.61	38.37	28.44	20.18	10.19	15.35	11.38
30/9 -B20	2,394	46.15	36.70	29.31	16.84	8.52	15.33	12.24
30/6-C04	2,631	52.39	40.44	26.12	26.27	12.06	15.37	9.93
30/6-C06	2,490	48.37	32.22	28.34	20.03	2.02	12.94	11.38
30/6-C10	2,535	49.44	35.55	28.23	21.21	7.05	14.02	11.13
30/6-C12	2,527	49.28	39.03	28.14	21.15	11.33	15.45	11.13
30/6-C20	2,500	48.61	38.00	27.96	20.65	9.80	15.20	11.18
30/6-C20	2,536	49.46	38.40	28.24	21.22	9.80	15.14	11.13
30/6-C20	2,470	47.93	38.20	28.11	19.82	10.40	15.47	11.38
30/6-C20B	2,681	52.86	40.05	26.06	26.80	9.85	14.94	9.72
30/9-6	2,567	50.31	44.10	28.33	21.98	14.70	17.18	11.04
30/9-7	2,756	54.58	46.10	26.77	27.81	14.80	16.73	9.71
30/9-B05A	2,463	48.78	36.20	28.03	20.75	8.50	14.70	11.38
306/7	2,900	57.75	49.20	28.16	29.59	15.93	16.97	9.71
30/6-17R	2,387	45.94	39.50	29.22	16.72	10.94	16.55	12.24
30/6-11	2,639	73.54	59.58	35.34	38.20	8.91	16.37	9.71

Table 5 Continued. Summary of in situ stress data from overburden rock in the Oseberg Field, North Sea

-21-

		Total Vertical Stress	Total Minimum Horizontal Stress	Pore Pressure	Effective Vertical Stress	Effective Horizontal Stress	Total Horizontal Stress Gradient	Pore Pressure Gradient
WELL	Depth (M)	(MPa)	(MPa)	(MPa)	(MPa)	(MPa)	(KPa/M)	(KPa/M)
1	3,235	76.67	66.24	60.76	15.92	5.48	20.48	18.78
2	3,196	75.76	46.82	27.78	47.98	19.05	14.65	8.69
3	3,450	81.77	77.57	74.38	7.40	3.19	22.49	21.56
4	3,302	78.26	51.28	29.51	48.75	21.76	15.53	8.94
5	3,600	85.34	63.55	37.79	47.55	25.76	17.65	10.50
6	3,631	86.07	82.71	75.17	10.91	7.54	22.78	20.70
7	3,679	87.19	61.95	29.81	57.38	32.13	16.84	8.10
8	3,807	90.23	88.00	78.03	12.20	9.97	23.12	20.50
9	3,355	79.52	71.64	64.82	14.69	6.82	21.36	19.32
10	3,513	83.27	76.78	71.70	11.57	5.08	21.85	20.41
11	3,604	85.49	79.08	76.63	8.86	2.44	21.94	21.27
12	3,669	86.98	79.36	75.72	11.26	3.64	21.63	20.63
13	3,713	88.02	82.07	75.75	12.27	6.32	22.10	20.40
14	3,635	86.16	78.04	72.04	14.11	5.99	21.47	19.82
9A	3,355	79.52	49.68	29.99	49.53	19.69	14.81	8.94
10A	3,513	83.27	49.89	22.13	61.14	27.76	14.20	6.30
11A	3,604	85.49	62.31	40.11	45.38	22.20	17.29	11.13
12A	3,669	86.98	59.73	18.97	68.01	40.76	16.28	5.17
13A	3,713	88.02	54.57	20.88	67.14	33.70	14.70	5.62
14A	3,635	86.16	51.12	16.16	69.99	34.95	14.06	4.45

Table 6. Summary of in situ stress data from the Vicksburg Formation, McAllen Ranch Field, Texas (From Salz, 1977)

Table 7. Summary of in situ stress data from Mesaverde Sandstone in the MWX-2 well of the Rulison Field, Colorado (From Warpinski and Teufel,1989)								
		Total Vertical Stress	Total Minimum Horizontal Stress	Pore Pressure	Effective Vertical Stress	Effective Horizontal Stress	· Total Horizontal Stress Gradient	Pore Pressure Gradient
Zone	Depth (M)	(MPa)	(MPa)	(MPa)	(MPa)	(MPa)	(KPa/M)	(KPa/M)
Cozzette	2,430	57.25	47.37	45.50	11.75	1.87	19.50	18.73
Cozzette	2,393	56.73	45.72	40.60	16.13	5.12	19.11	16.97
Rollins	2,295	54.43	45.35	38.20	16.23	7.15	19.75	16.64
Rollins	2,276	53.95	46.79	26.80	27.15	19.99	20.56	11.78
Paludal	2,254	53.43	46.24	34.00	19.43	12.24	20.51	15.08
Paludal	2,216	52.52	43.35	25.50	27.02	17.85	19.56	11.51
Paludal	2,170	51.44	40.60	24.10	27.34	16.50	18.71	11.11
Paludal	2,123	50.31	39.53	25.50	24.81	14.03	18.62	12.01
Coastal	1,996	48.21	38.81	33.80	14.41	5.01	19.44	16.93
Coastal	1,985	47.95	40.22	26.40	21.55	13.82	20.26	13.30
Coastal	1,969	47.57	39.01	26.20	21.37	12.81	19.81	13.30
Coastal	1,964	47.44	39.36	28.90	18.54	10.46	20.04	14.72
Fluvial	1,818	43.90	31.65	27.40	16.50	4.25	17.41	15.08
Fluvial	1,779	42.96	31.65	26.70	16.26	4.95	17.80	15.01
Fluvial	1,744	42.12	31.48	27.20	14.92	4.28	18.05	15.60
Fluvial	1,686	40.71	31.31	28.80	11.91	2.51	18.57	17.09
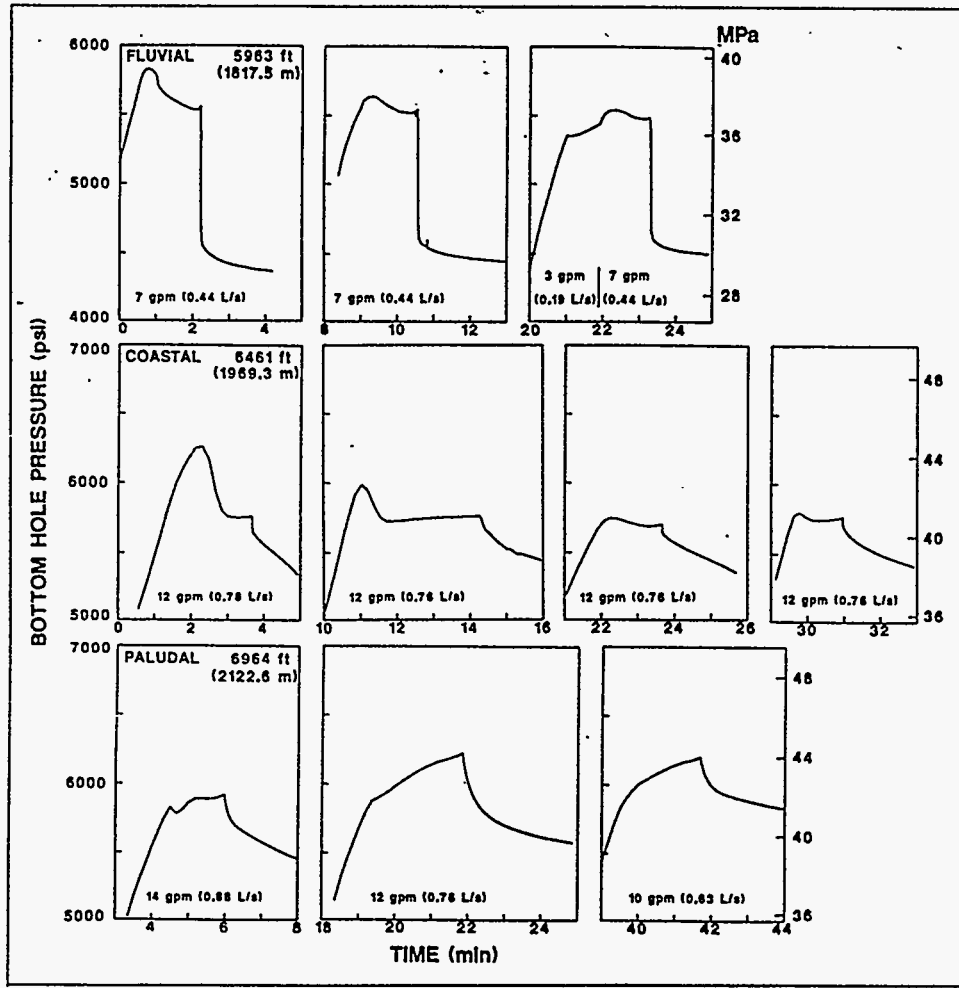
Figure 1. Example minifracture pressure records for sandstones from Mesaverde Formation in the Rulison Field, Colorado (from Warpinski and Teufel, 1989).
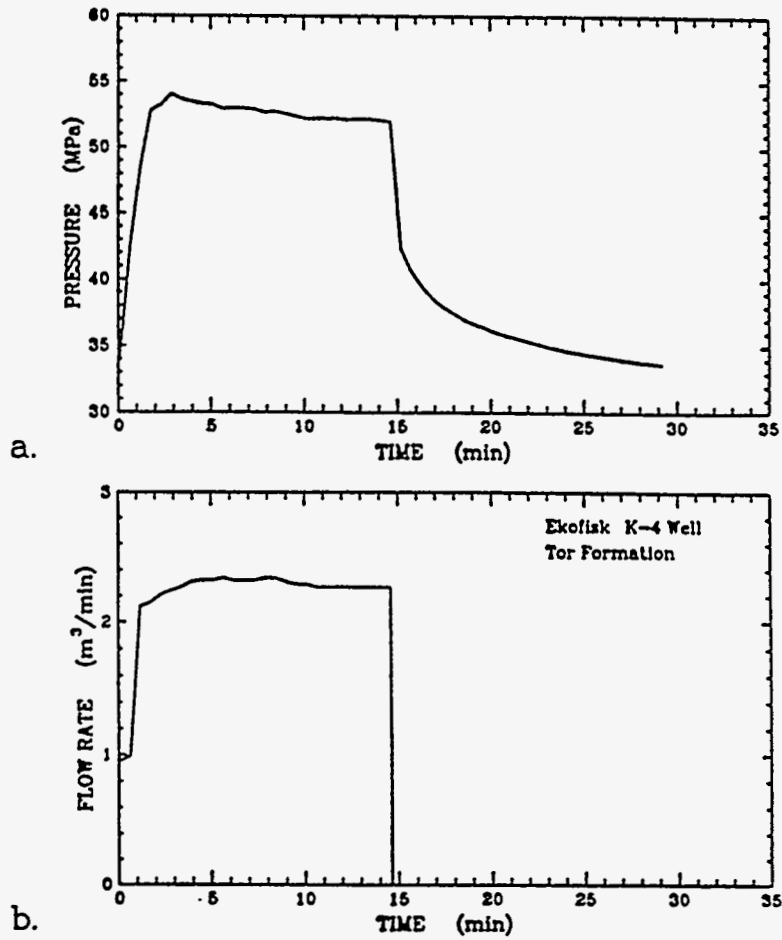
Figure 2. (a) Plot of pressure versus time of a hydraulic fracture treatment in the 2/4 K5 well in the Ekofisk Field showing the breakdown and shut-in at the completion of the first phase of the stimulation treatment. (b) Plot of flow rate versus time.
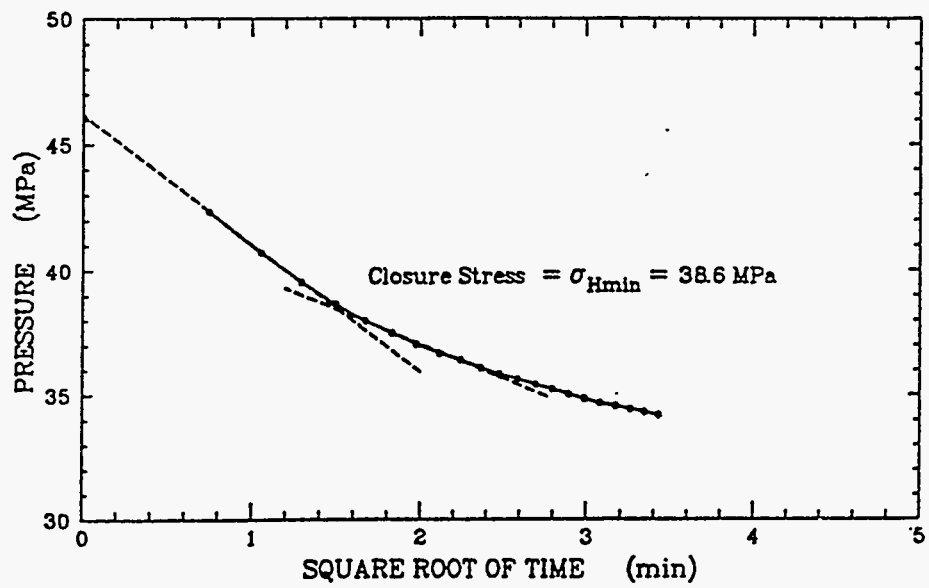
Figure 3. Plot of pressure versus square root of time for shut-in data for the 2/4 K-5 well in the chalk reservoir at the Ekofisk Field.
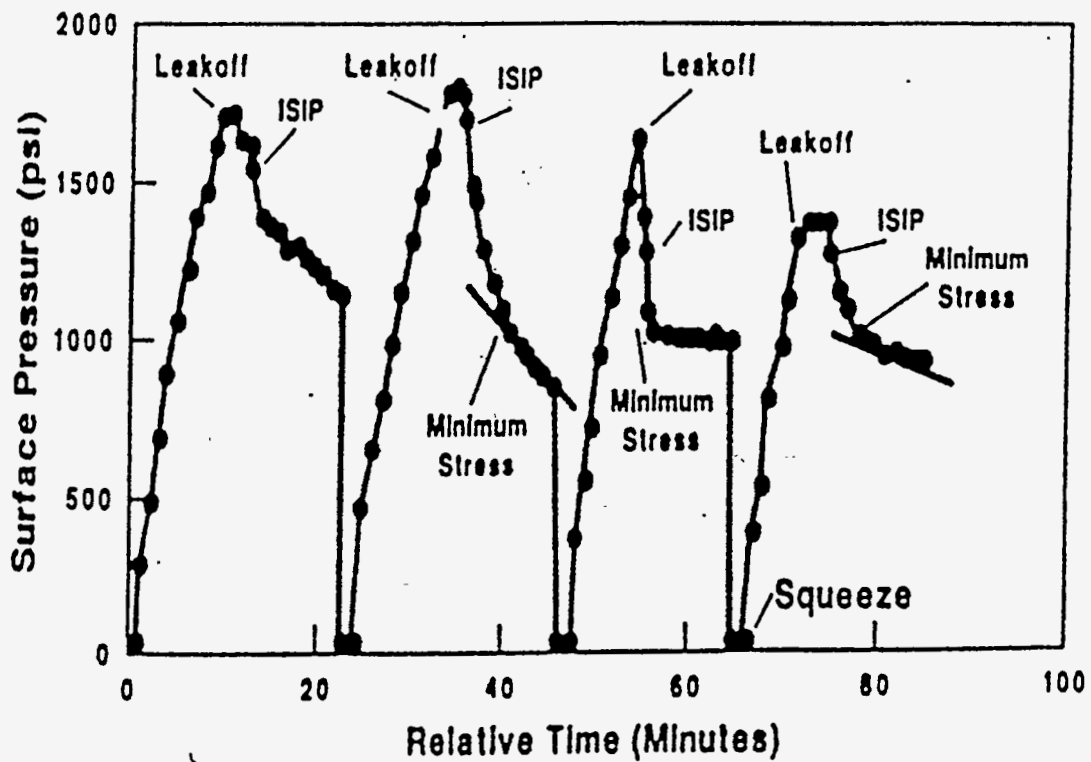
Figure 4. An example of an extended leak-off test (from Kunze and Steiger, 1992)
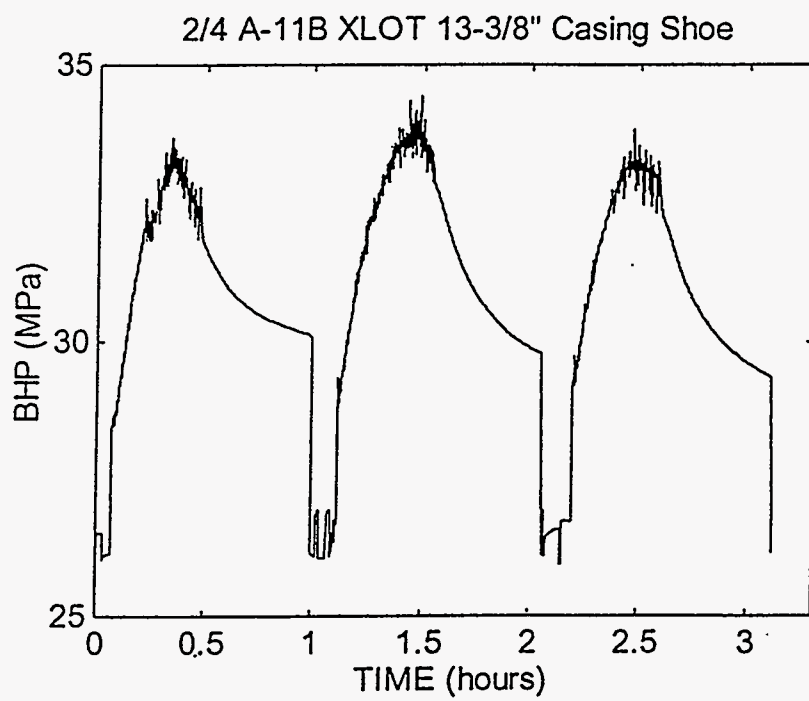
Figure 5. Bottomhole pressure (BHP) versus time for an extended leak-off test in the 2/4 A-11b well in overburden rock at Ekofisk Field.
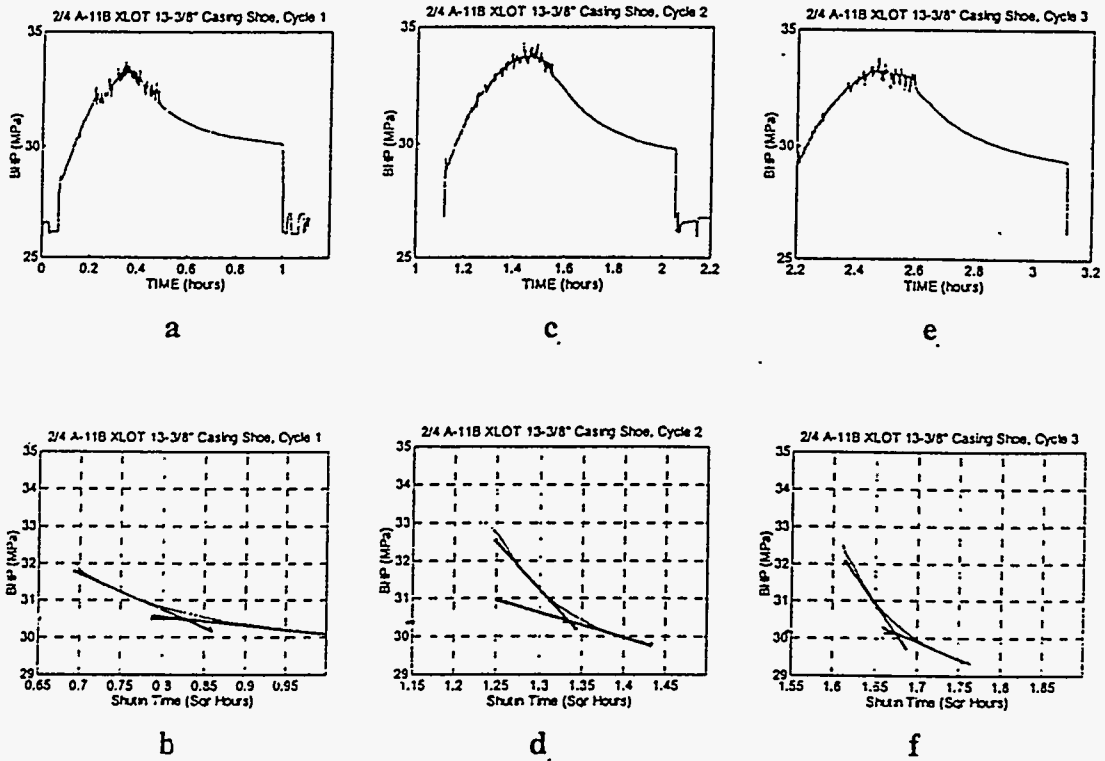
Figure 6. Plots showing each extended leak-off test cycle in the 2/4 A-11B well in the overburden rock at Ekofisk Field and corresponding plots of bottomhole pressure (BHP) versus square root of time for shut-in to determine fracture closure pressure.
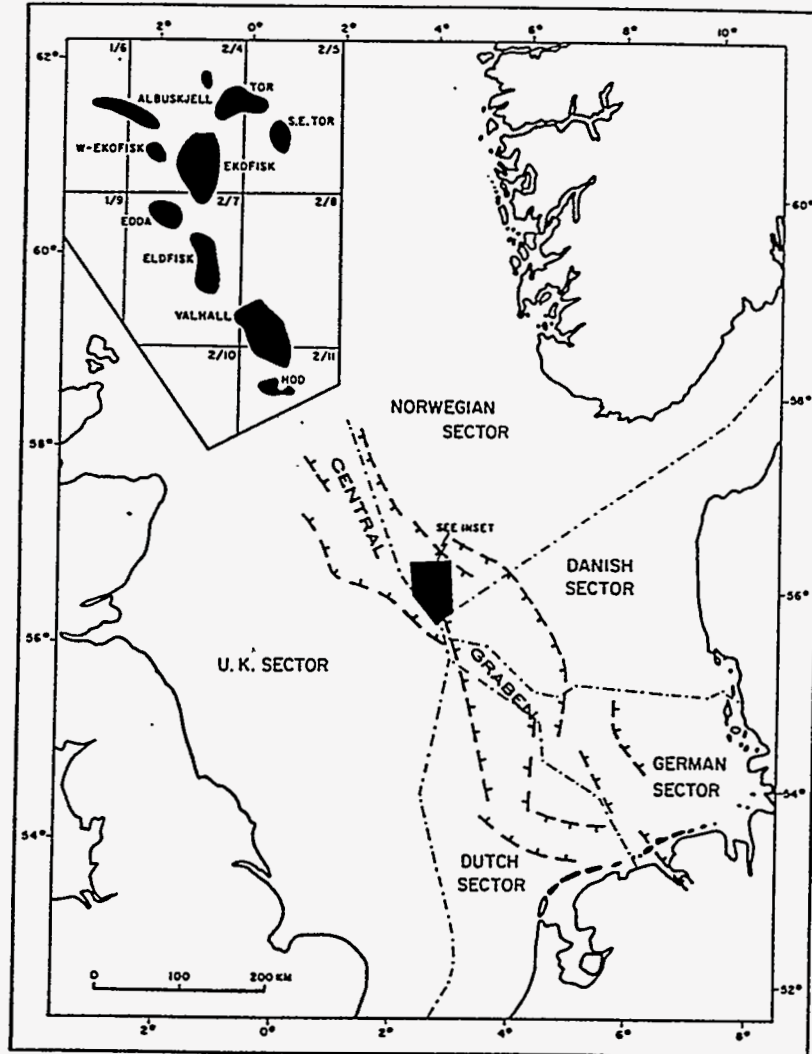
Figure 7. Map of southern part of the North Sea showing the location of chalk reservoirs in the central graben.

Valhall Field, North Sea
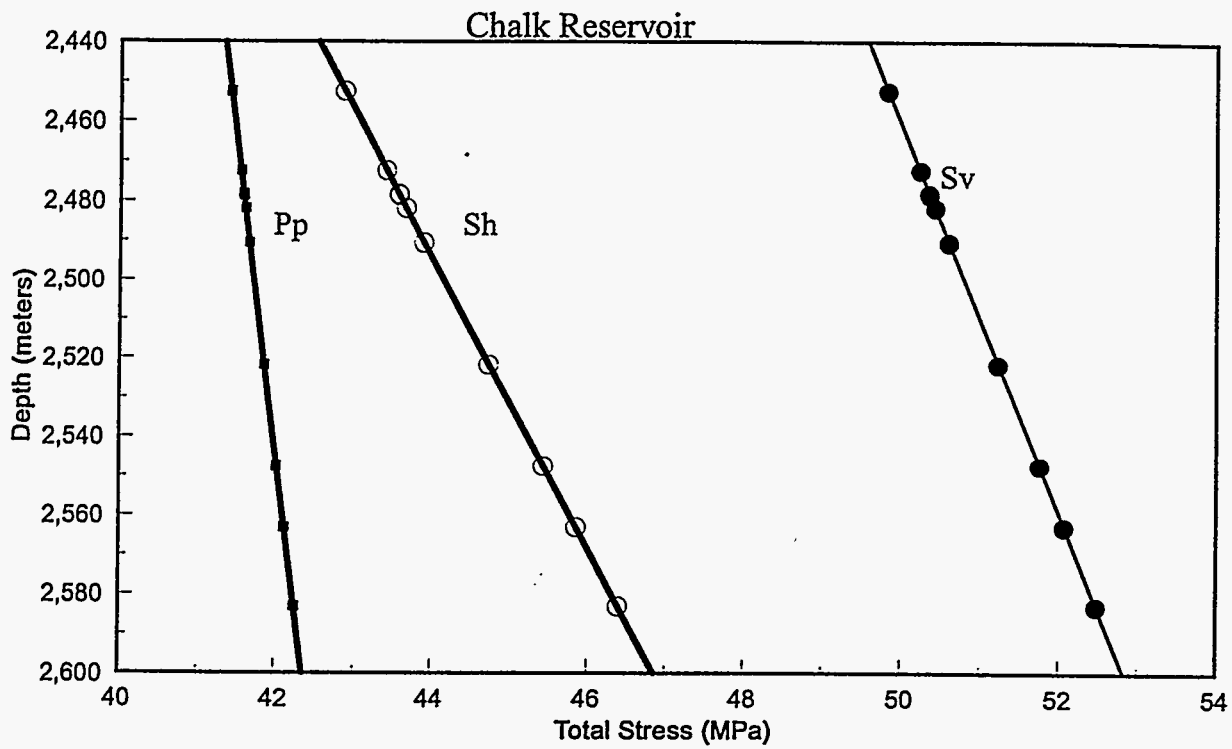
Chalk Reservoir

Figure 8. Plot of total vertical stress, total minimum horizontal stress and pore pressure versus depth for chalk reservoirs in the Valhall Field before production.

Figure 9. Plot of effective vertical stress versus minimum effective horizontal stress for chalk reservoirs in the Valhall Field, North Sea before production.

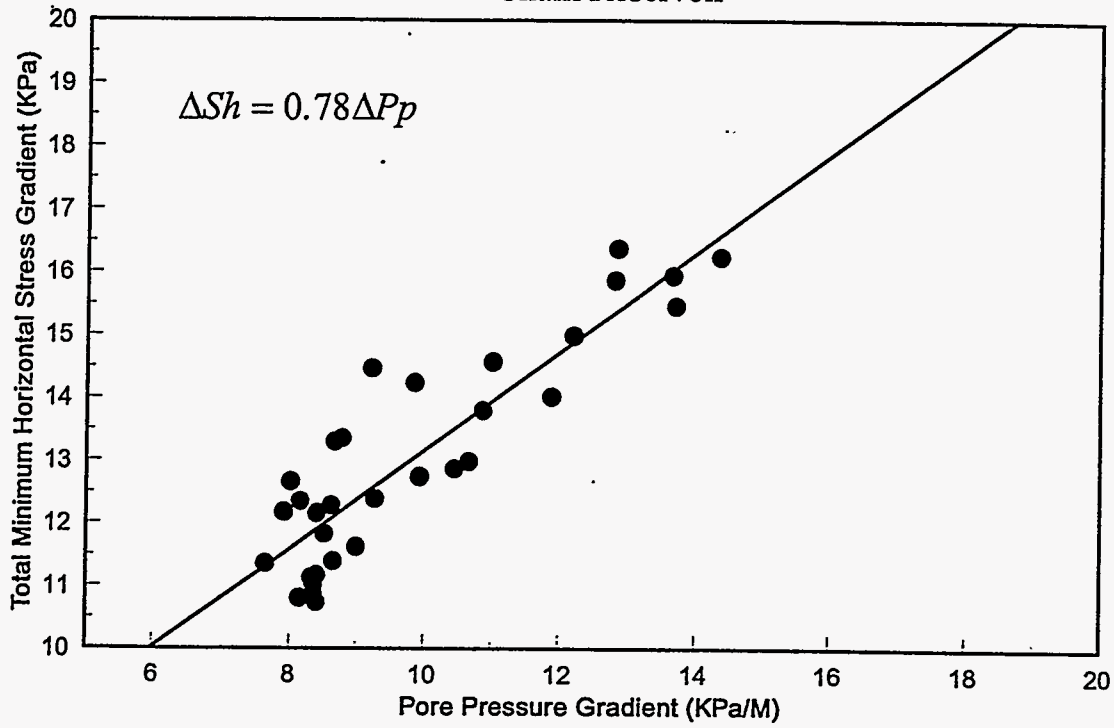Figure 10. Plot of pore pressure versus total minimum horizontal stress for chalk reservoirs in the Valhall Field, North Sea before and after production.

Valhall Field, North Sea
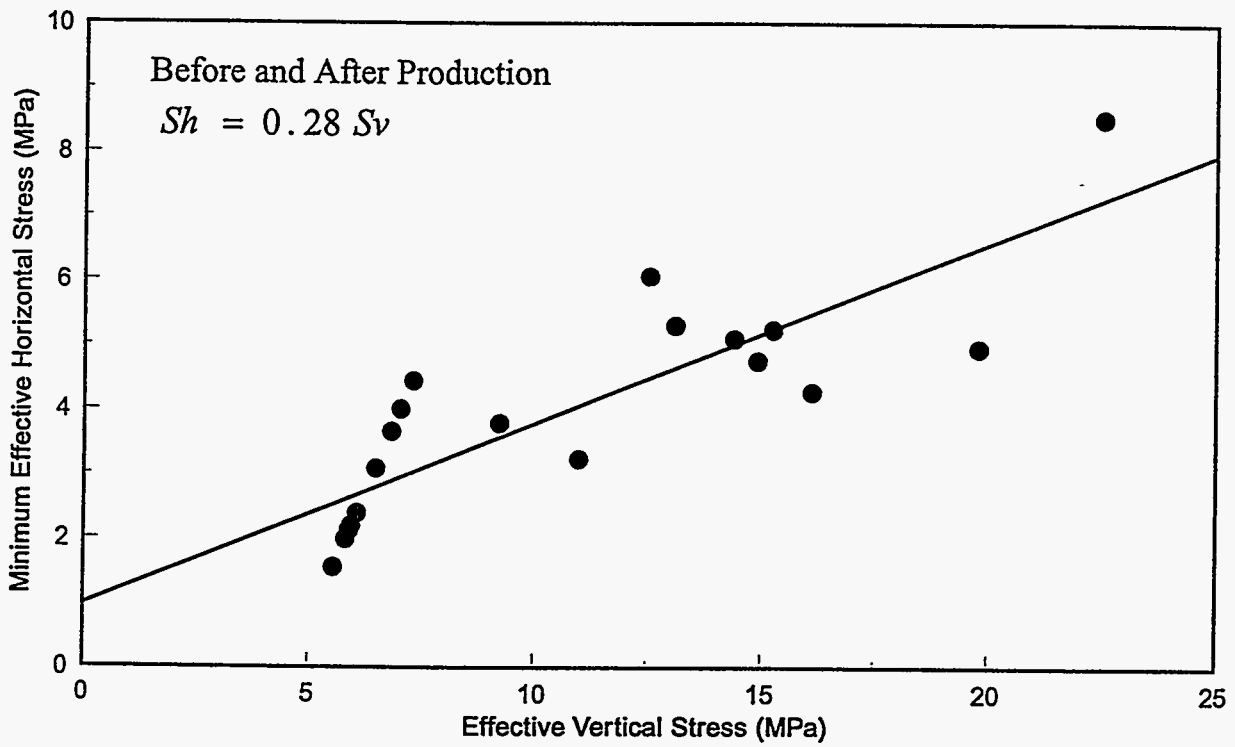
Chalk Reservoir

Figure 11. Plot of effective vertical stress versus minimum effective horizontal stress for chalk reservoirs in the Valhall Field, North Sea before and after production.

Eldfisk Field, North Sea
Chalk Reservoir

$$Sh = 0.86\ Pp$$
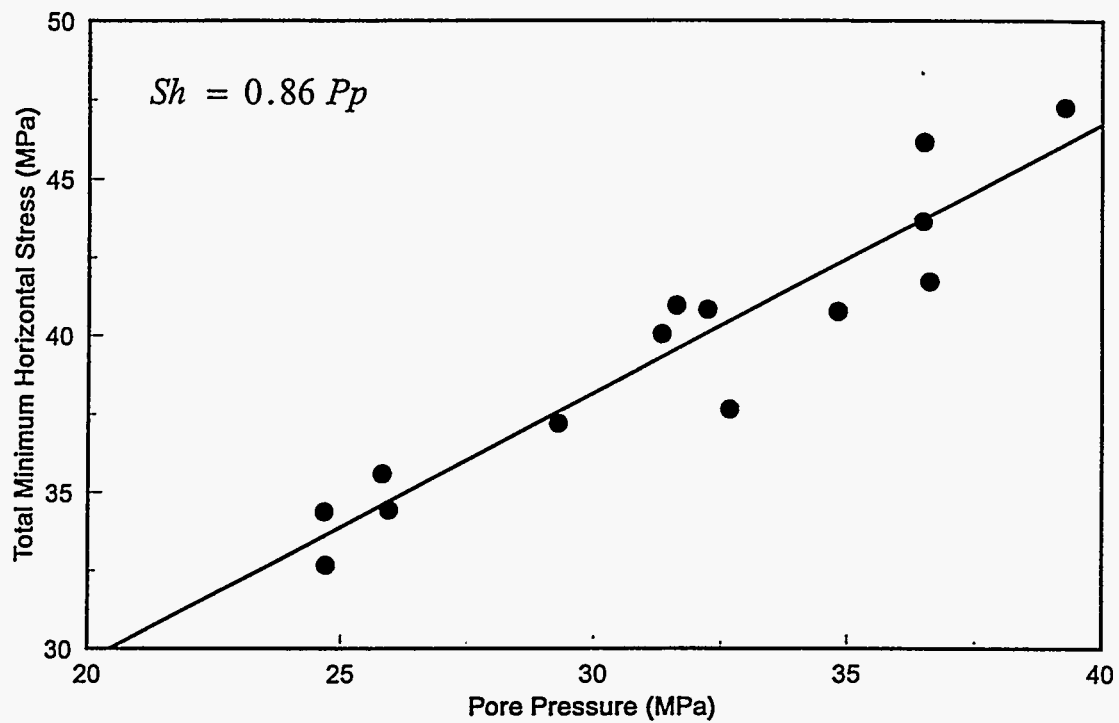
Figure 12. Plot of pore pressure versus total minimum horizontal stress for chalk reservoirs in the Eldfisk Field, North Sea. Change in pore pressure is caused by production.
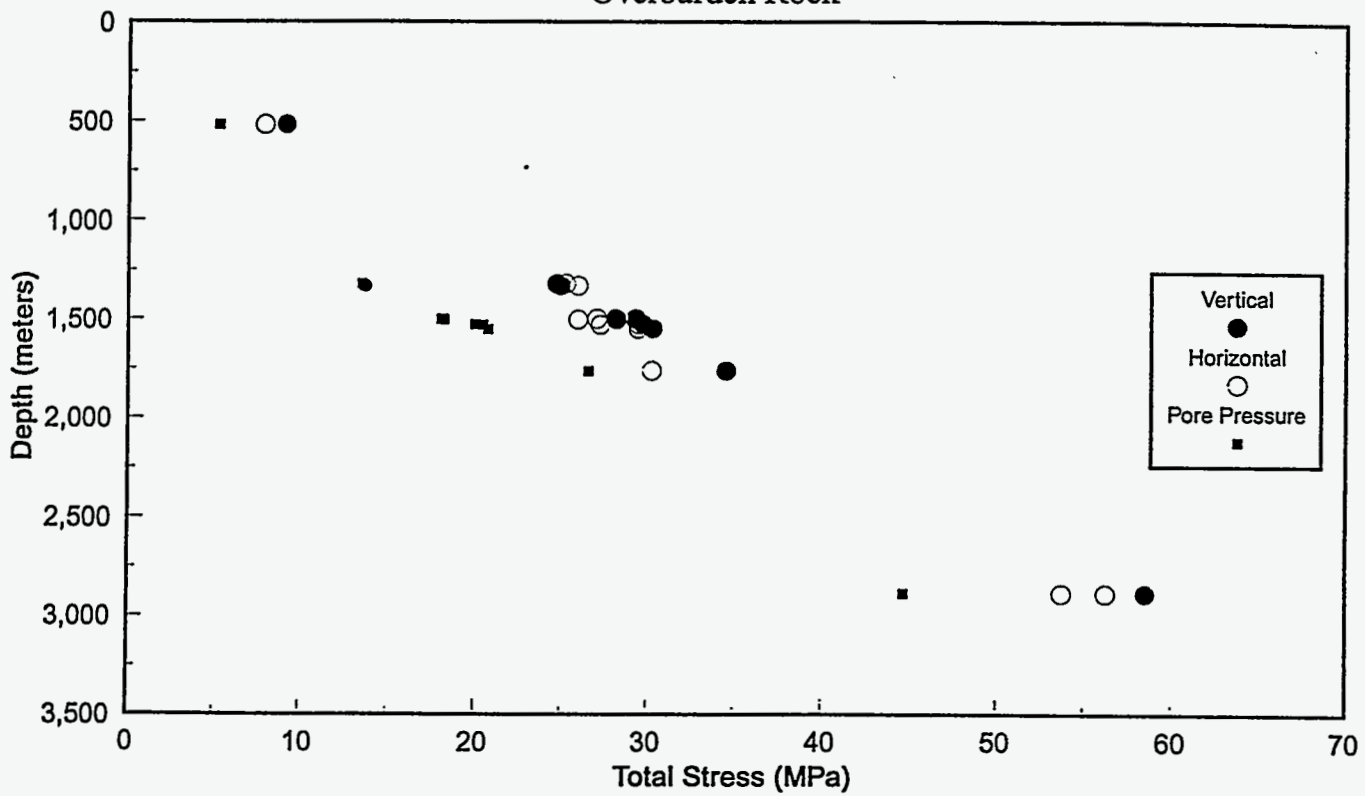
Eldfisk Field , North Sea

Chalk Reservoir

$$\Delta Sh = 0.84 \Delta Pp$$
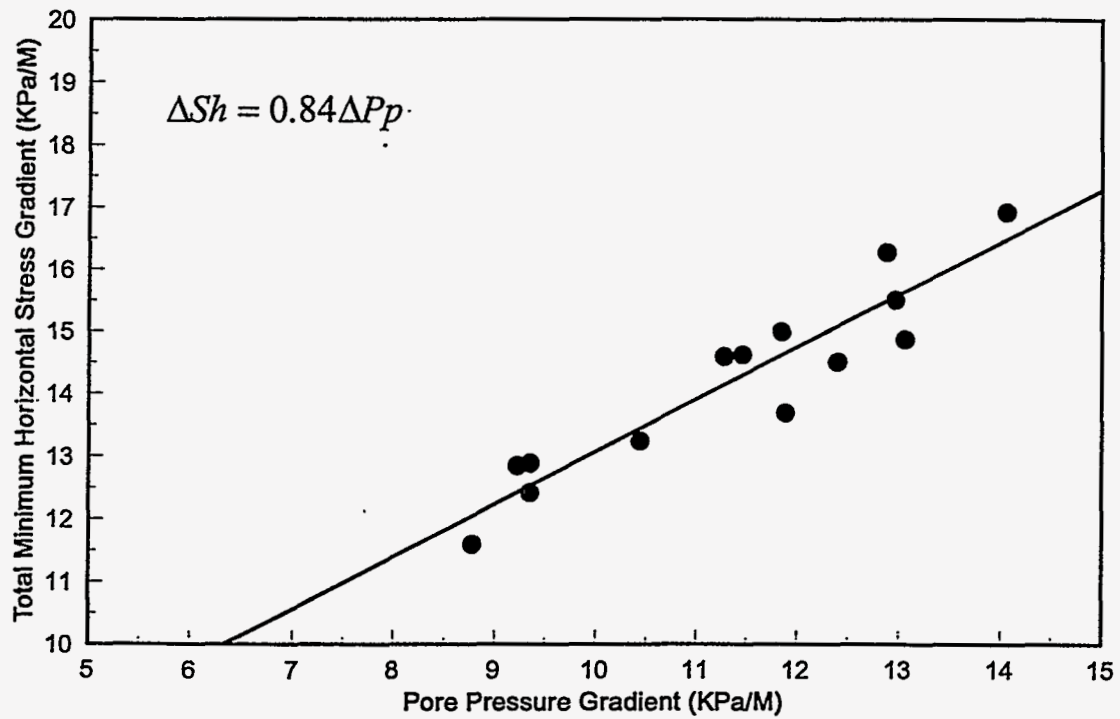
Figure13. Plot of pore pressure gradient versus total minimum horizontal stress for chalk reservoirs in the Eldfisk Field, North Sea. Change in pore pressure is caused by production.
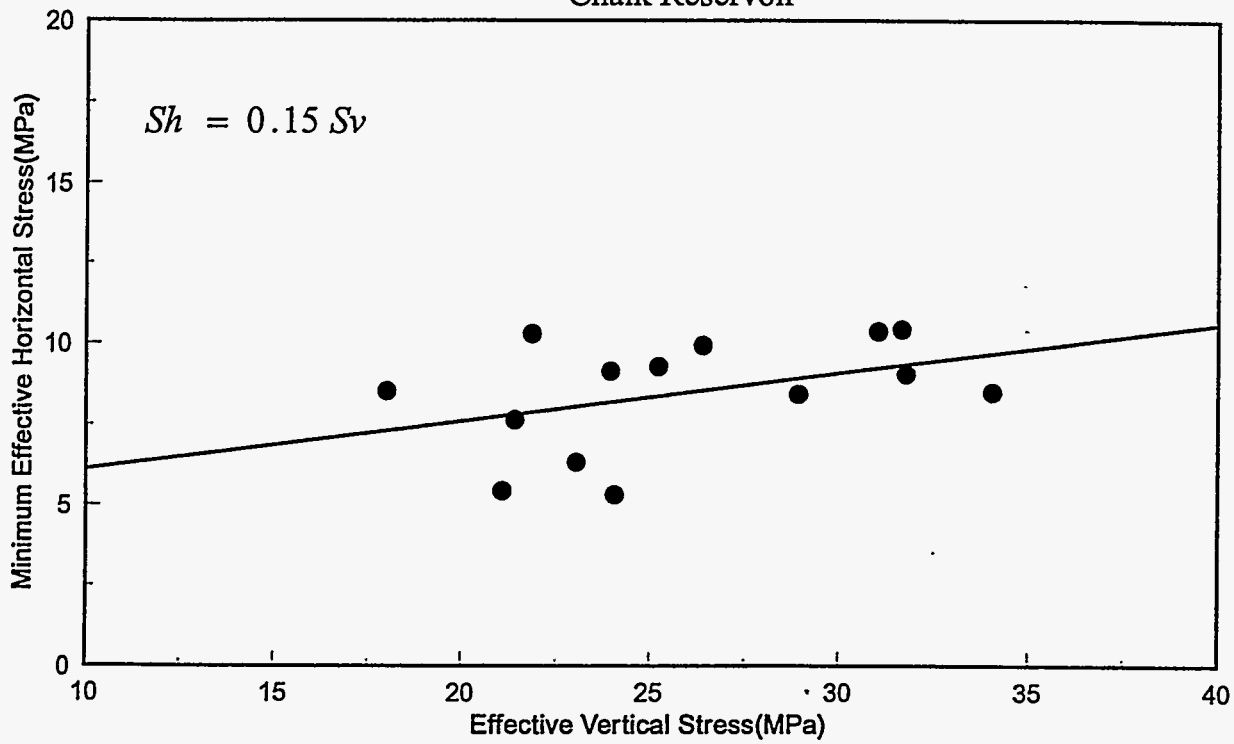
Figure 14. Plot of effective vertical stress versus minimum effective stress for chalk reservoirs in the Eldfisk Field, North Sea.
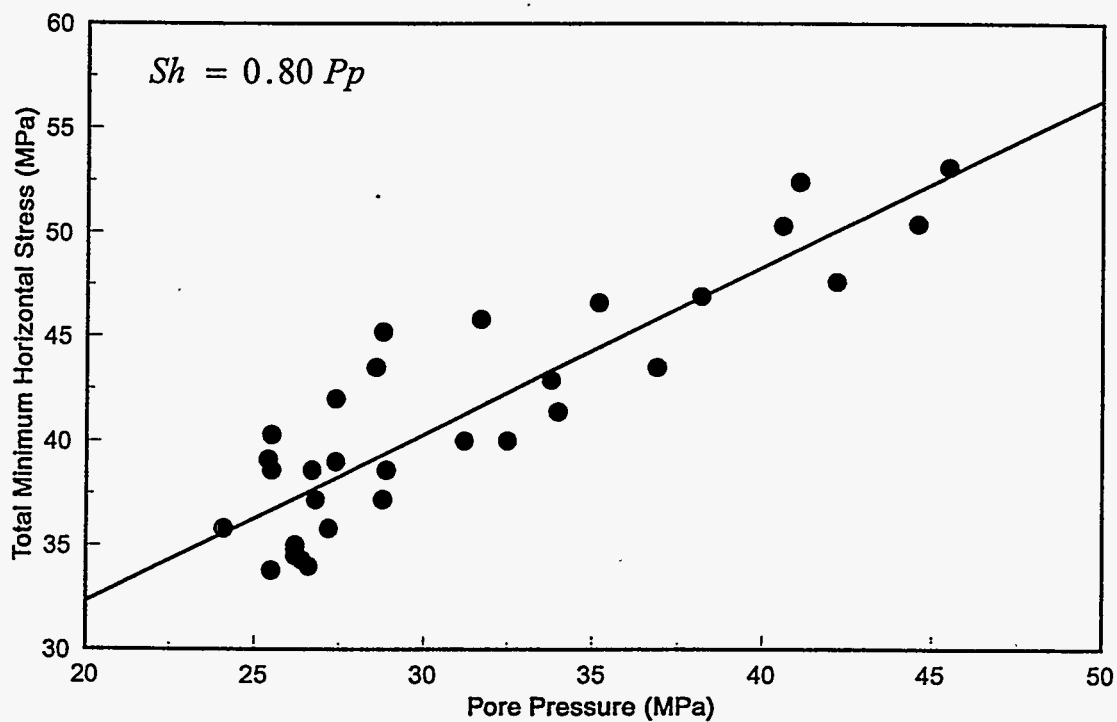
Figure 15. Plot of pore pressure versus total minimum horizontal stress for
chalk reservoirs in the Ekofisk Field, North Sea. Change in
pore pressure is caused by production.

Ekofisk Field, North Sea

Chalk Reservoir

Figure 16. Plot of pore pressure gradient versus total minimum horizontal stress gradient for chalk reservoirs in the Ekofisk Field, North Sea. Change in pore pressure is caused by production.

Ekofisk Field North Sea

Chalk Reservoir

$Sh = 0.22 \, Sv$

(Plot: x-axis "Effective Vertical Stress (MPa)" from 15 to 45; y-axis "Minimum Effective Horizontal Stress (MPa)" from 0 to 20)

Figure 17. Plot of effective vertical stress versus minimum effective stress for chalk reservoirs in the Ekofisk Field, North Sea. Change in pore pressure is caused by production.

Ekofisk Field, North Sea

Overburden Rock

Figure 18. Plot of total vertical stress, total minimum horizontal stress, and pore pressure versus depth for the overburden rock in the Ekofisk Field, North Sea.
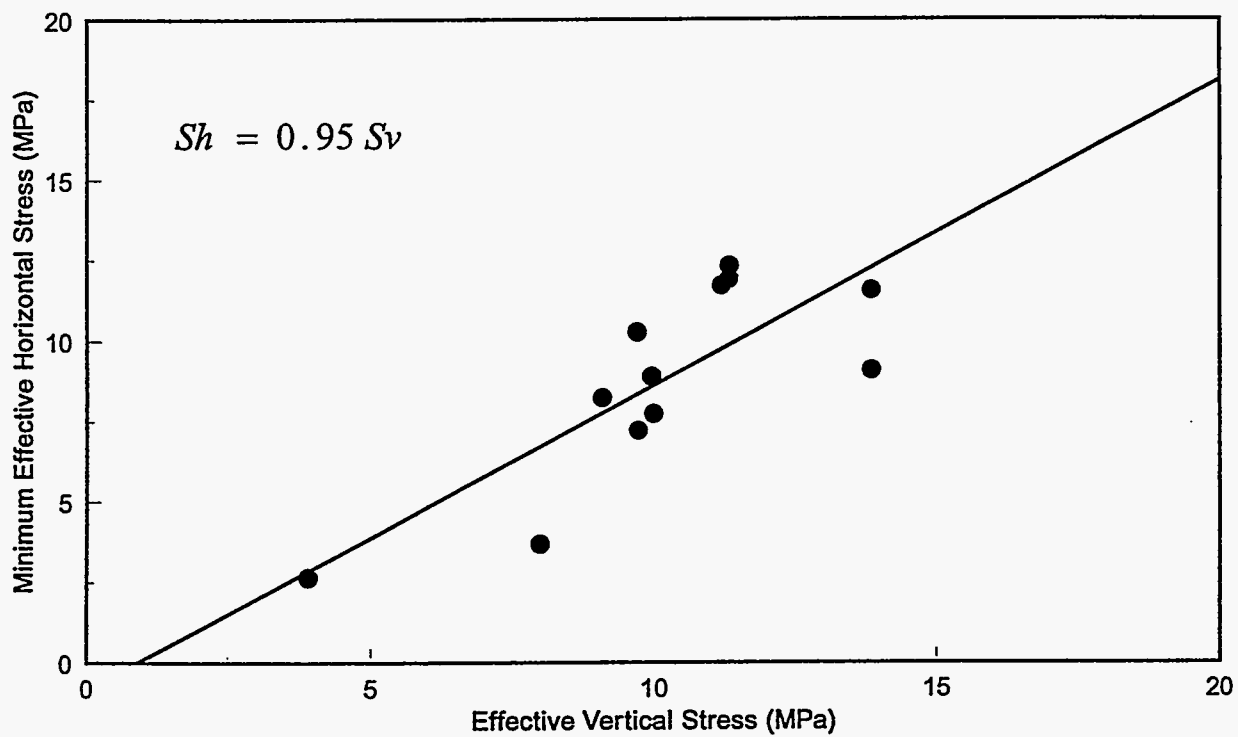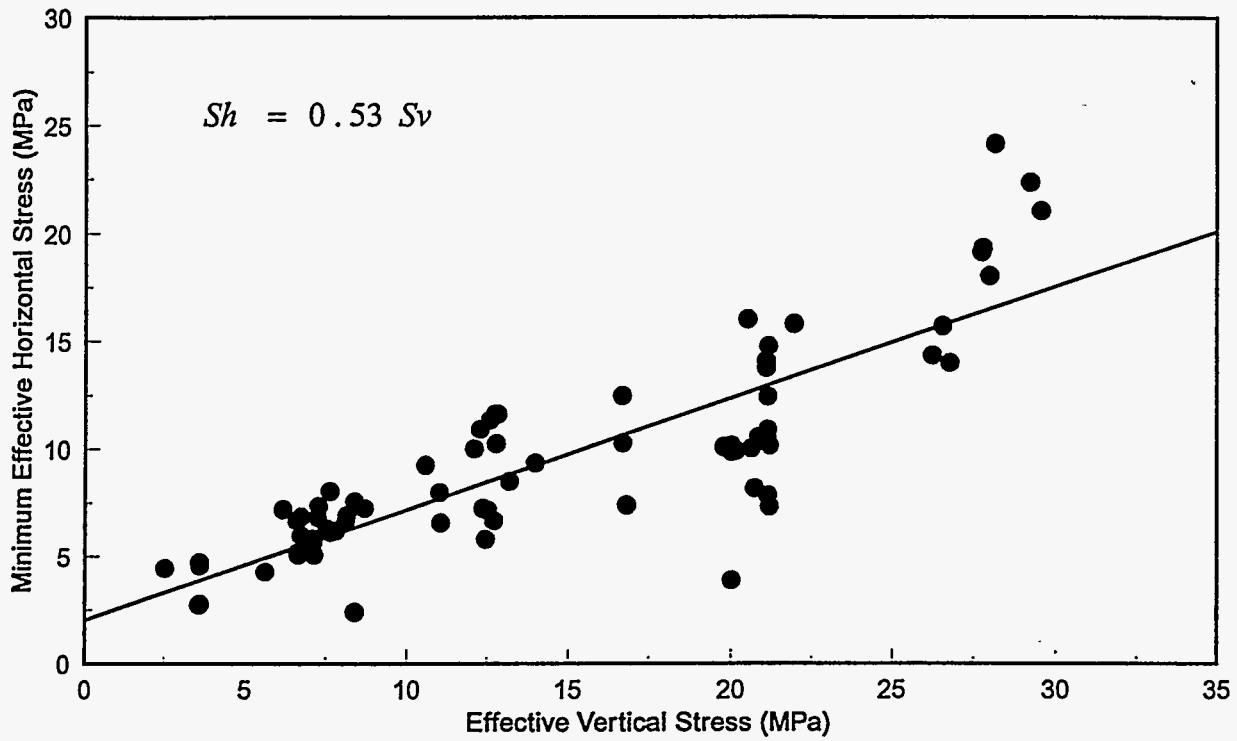
Figure 19. Plot of effective vertical stress versus minimum effective horizontal stress for the overburden rock in the Ekofisk Field, North Sea.

Oseberg Field, North Sea
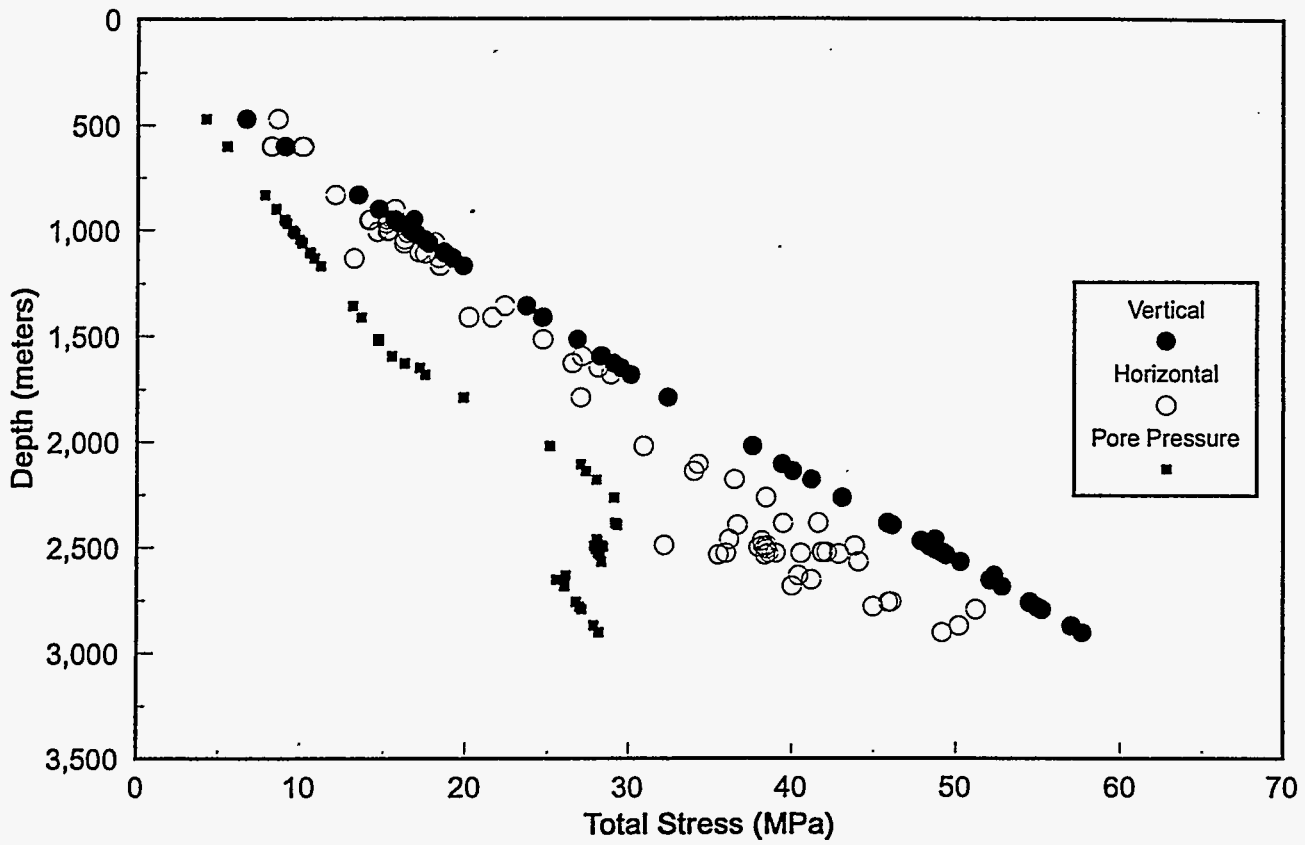
Overburden Rock

Figure 20. Plot of total vertical stress, total minimum horizontal stress and pore pressure versus depth for the overburden rock in the Oseberg Field, North Sea.

Oseberg Field, North Sea
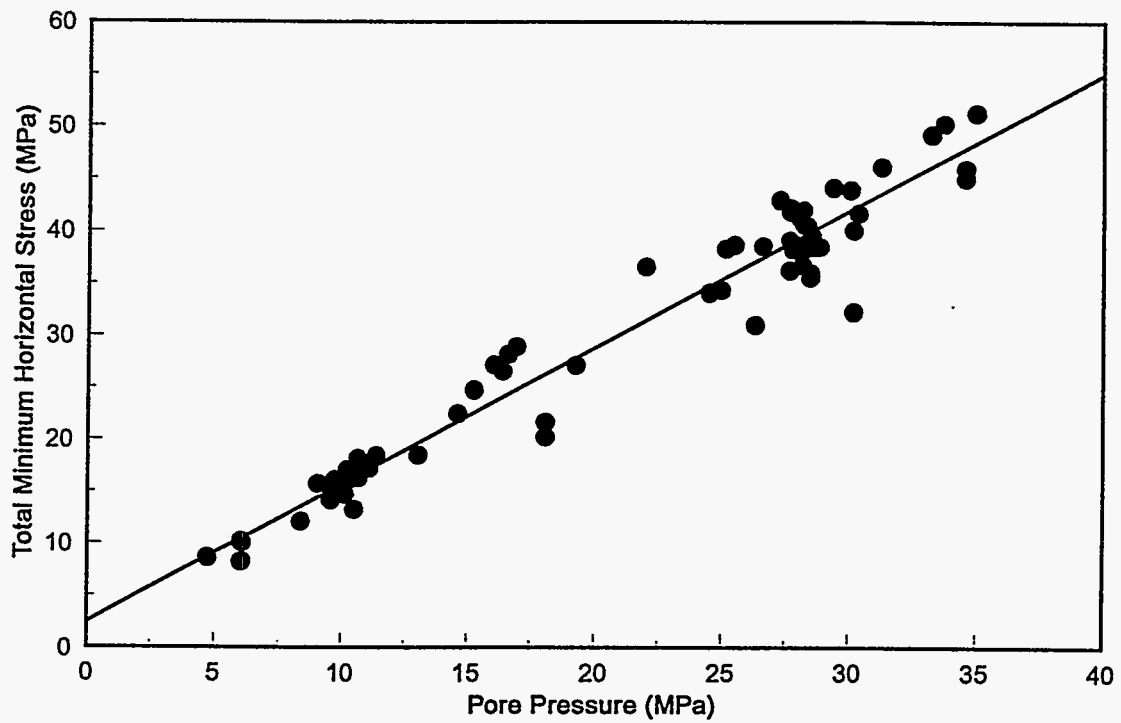
Overburden Rock

Figure 21. Plot of pore pressure versus total minimum horizontal stress for the overburden rock in the Oseberg Field, North Sea.

Oseberg Field, North Sea
Overburden Rock

Figure 22. Plot of effective vertical stress versus minimum effective horizontal stress for the overburden rock in the Oseberg Field, North Sea.

McAllen Ranch Field, Texas

Vicksburg Formation

Before Production

$$Sh = 0.57\ P\dot{p}$$
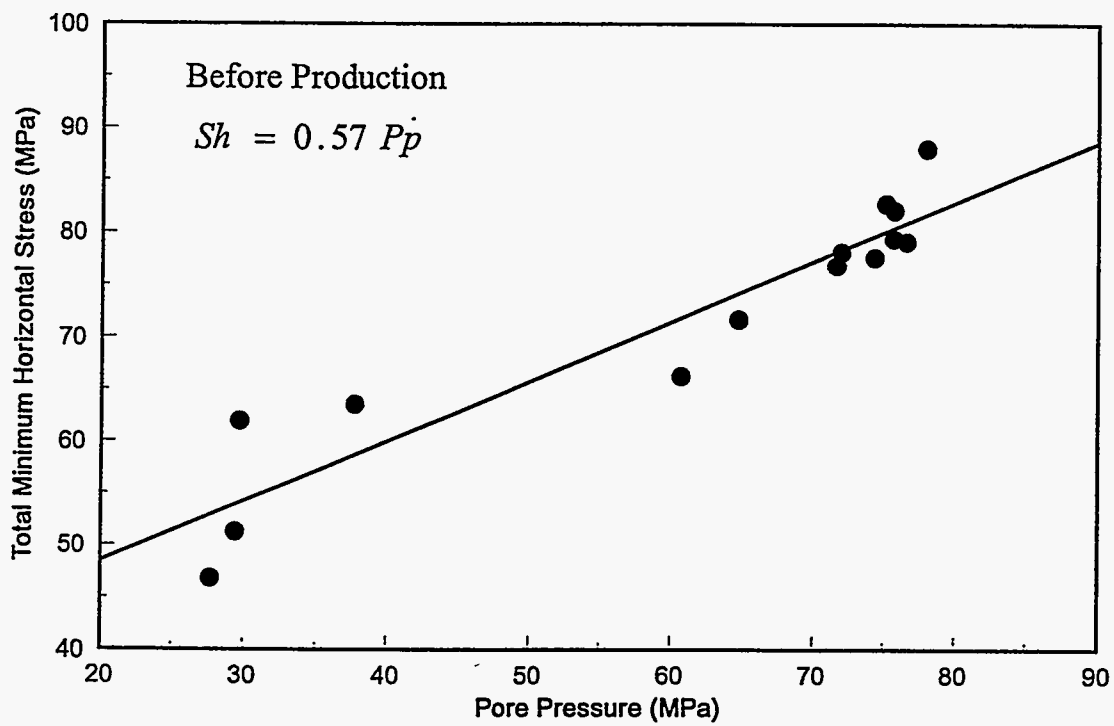
Figure 23. Plot of pore pressure versus total minimum horizontal stress for the Vicksburg Formation in the McAllen Ranch Field, Texas.

McAllen Ranch Field, Texas

Vicksburg Formation

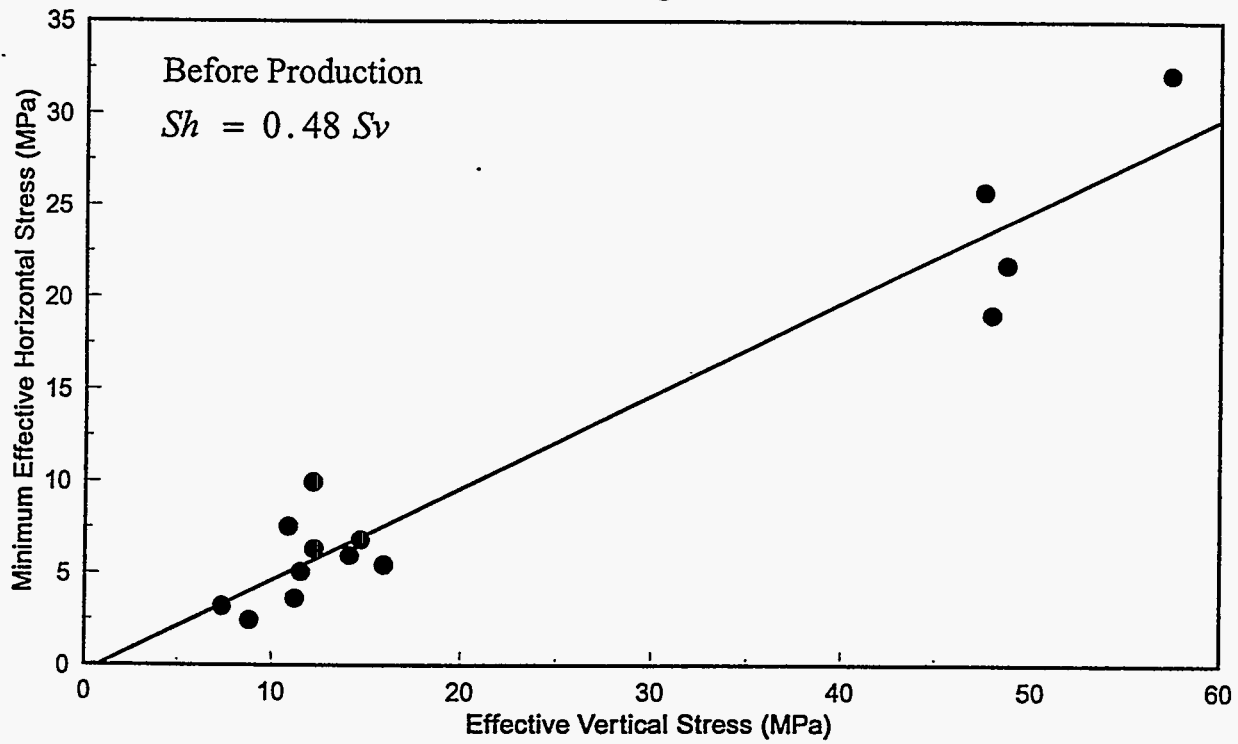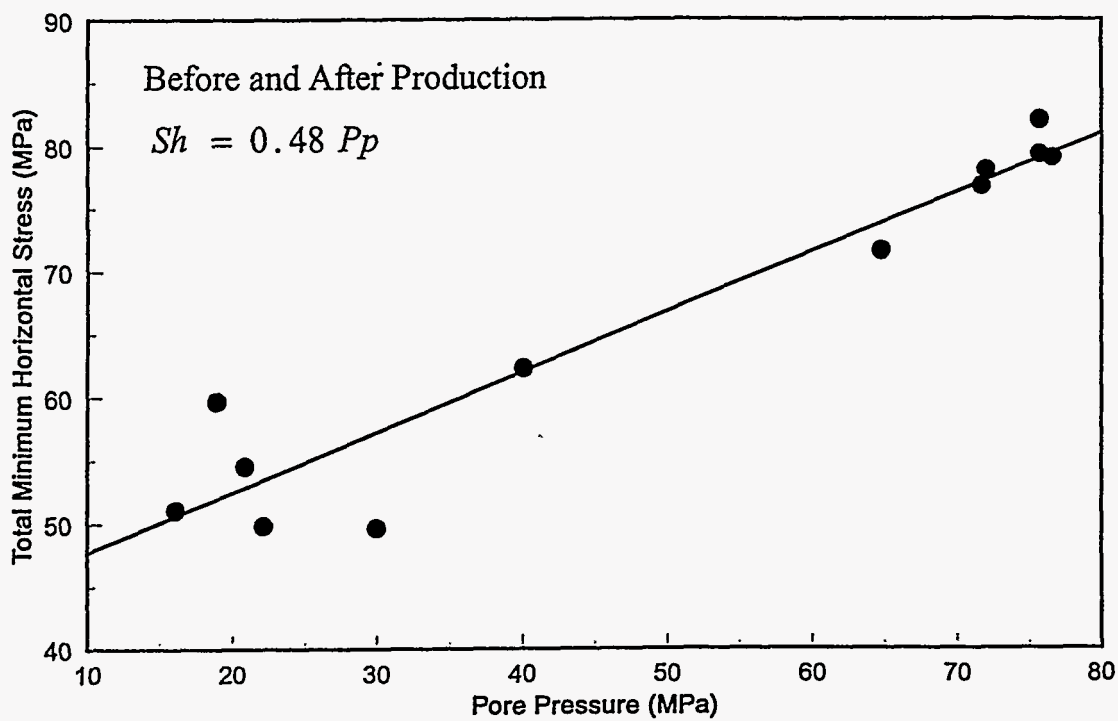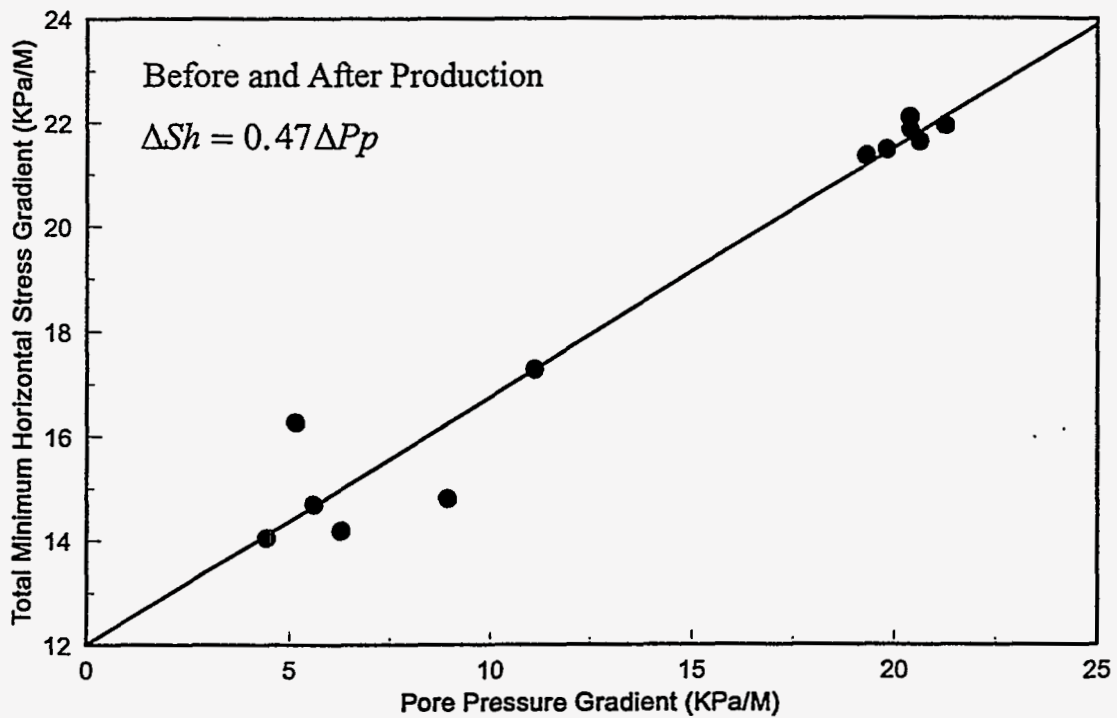Before Production
$$\Delta Sh = 0.54 \Delta Pp$$
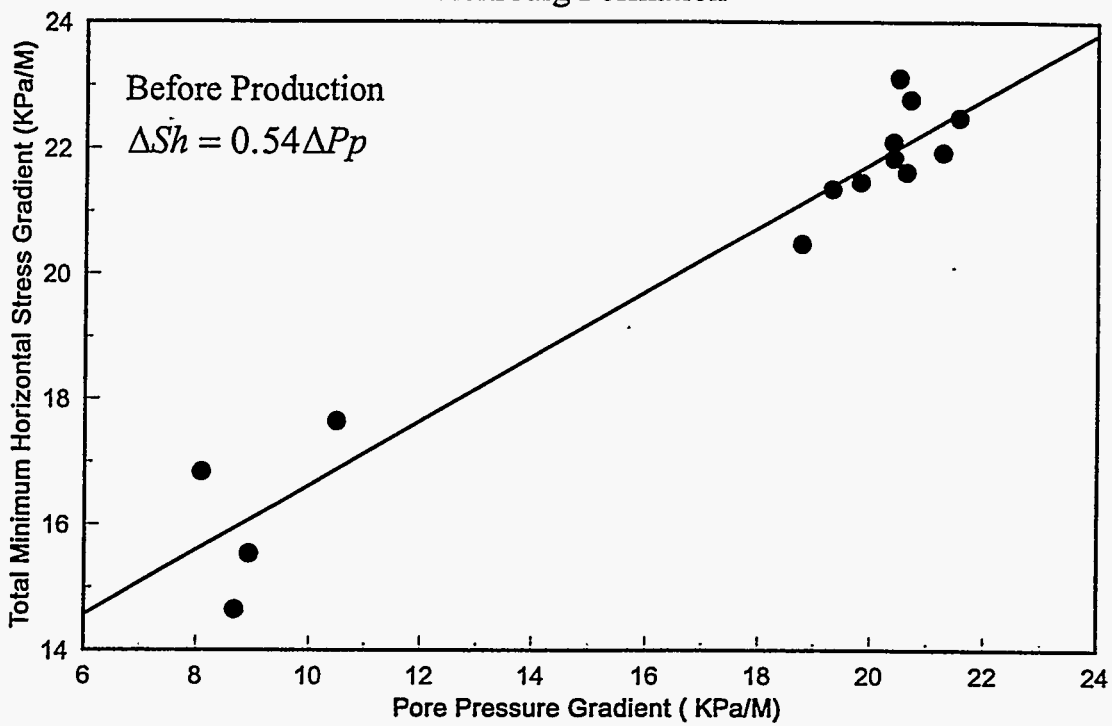
Figure 24. Plot of pore pressure gradient versus total minimum horizontal stress gradient for theVicksburg Formation in the McAllen Ranch Field, Texas.

McAllen Ranch Field, Texas
Vicksburg Formation

Before Production

$Sh = 0.48\ Sv$

Figure 25. Plot of effective vertical stress versus minimum effective horizontal stress for the Vicksburg Formation in the McAllen Field, Texas.

McAllen Ranch Field, Texas

Vicksburg Formation

Before and After Production

$$Sh = 0.48 \, Pp$$

Y-axis: Total Minimum Horizontal Stress (MPa)
X-axis: Pore Pressure (MPa)

Figure 26. Plot of pore pressure versus total minimum horizontal stress for the Vicksburg Formation in the McAllen Ranch Field, Texas.

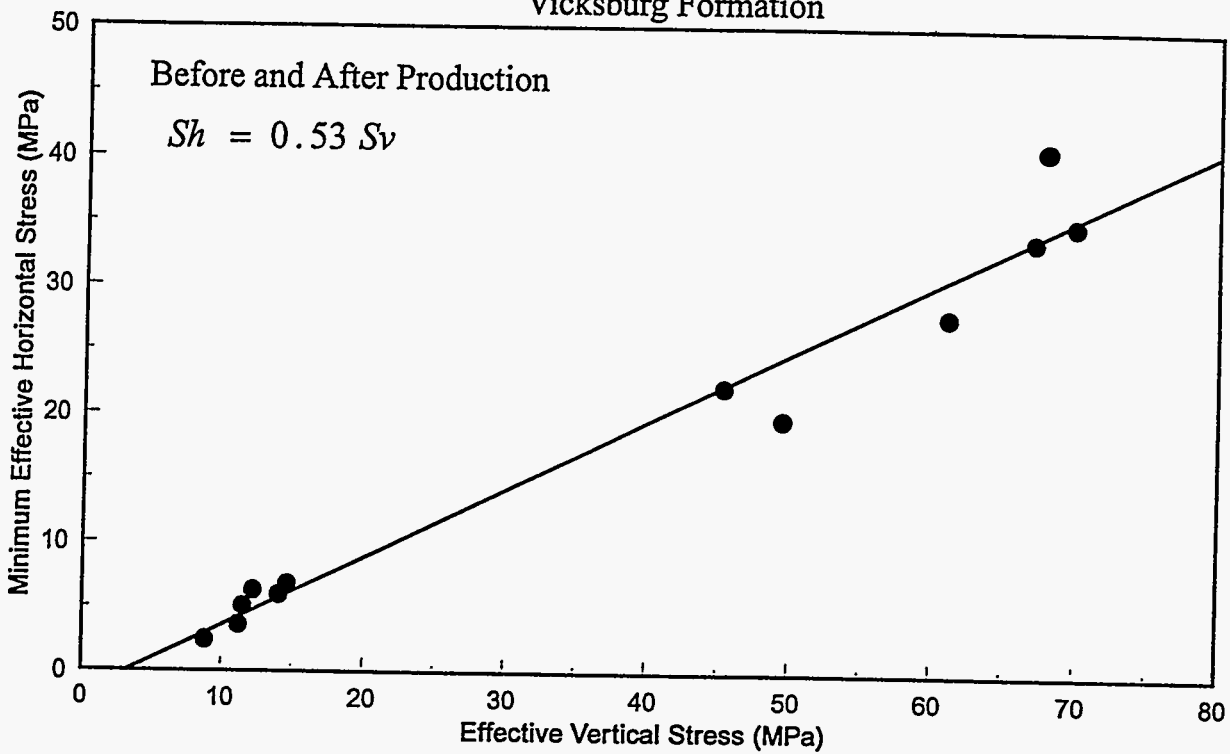# McAllen Ranch Field, Texas

Vicksburg Formation

Before and After Production

$\Delta Sh = 0.47 \Delta Pp$

Figure 27. Plot of pore pressure gradient versus total minimum horizontal stress for the Vicksburg Formation in the McAllen Ranch Field, Texas.

Figure 28. Plot of effective vertical stress versus minimum effective horizontal stress for the Vicksburg Formation in the McAllen Field, Texas.

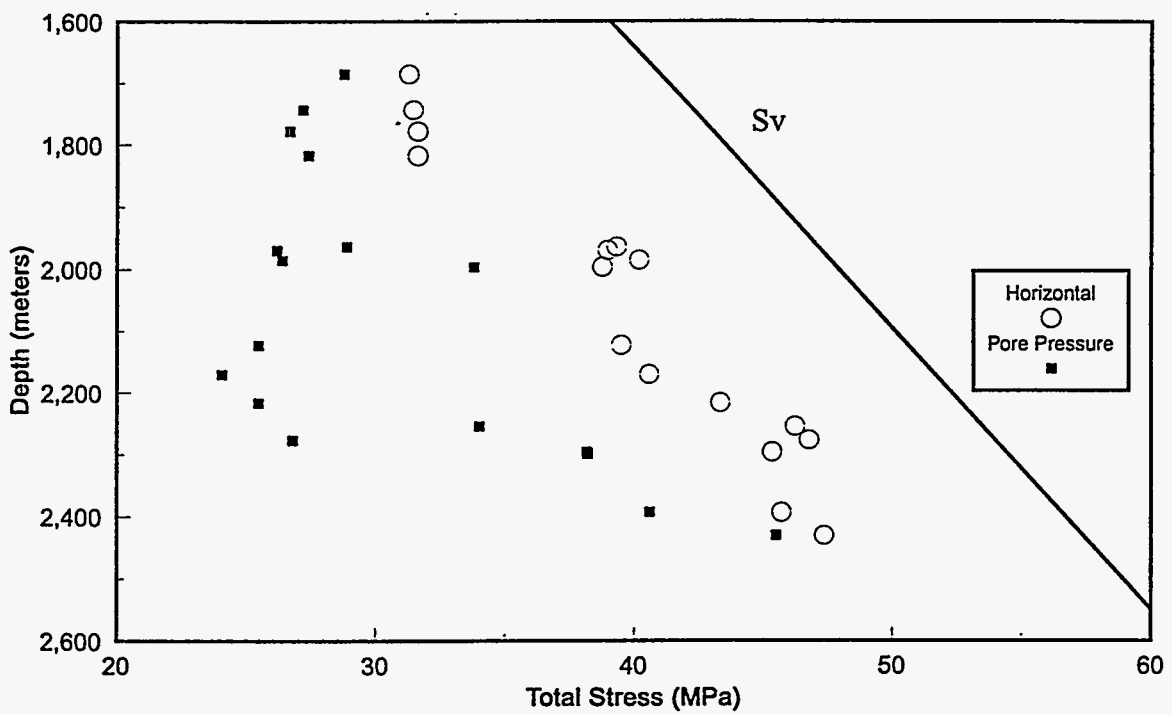# Rulison Field, Colorado

Mesaverde Sandstone

Figure 29. Plot of total vertical stress, total minimum horizontal stress and pore pressure versus depth for the Mesaverde sandstone in the Rulison Field, Colorado.

Rulison Field, Colorado

Mesaverde Sandstone
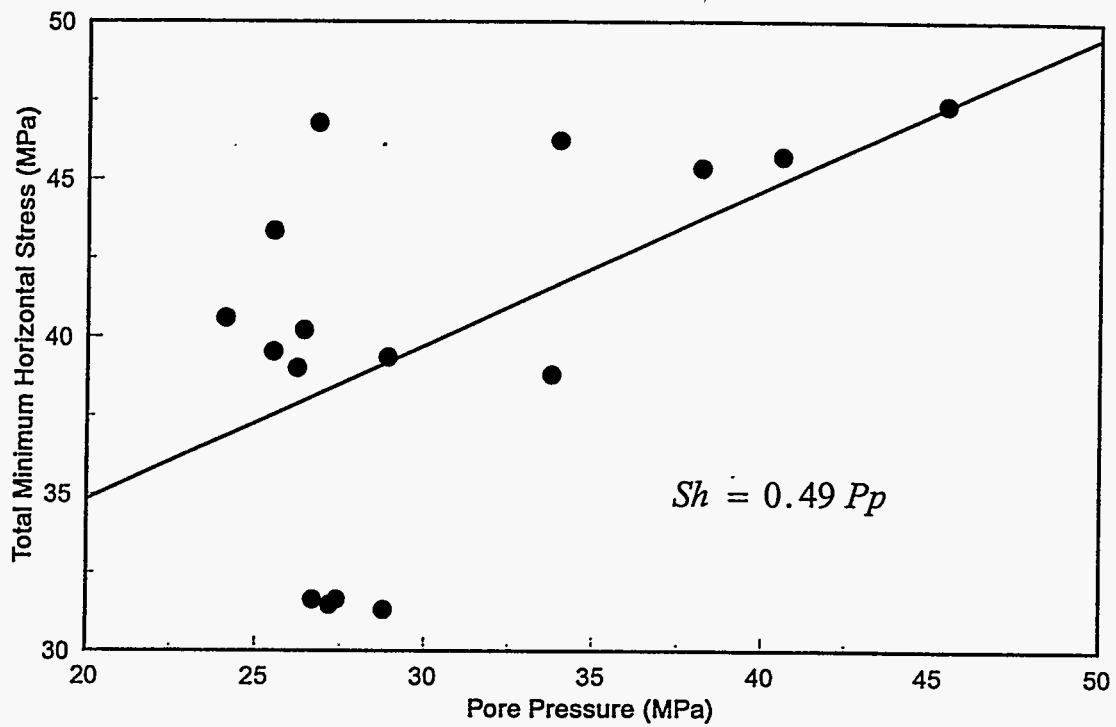

$$Sh = 0.49 \, Pp$$

Figure 30. Plot of pore pressure versus total minimum horizontal stress for the Mesaverde sandstone in the Rulison Field, Colorado.

Rulison Field, Colorado
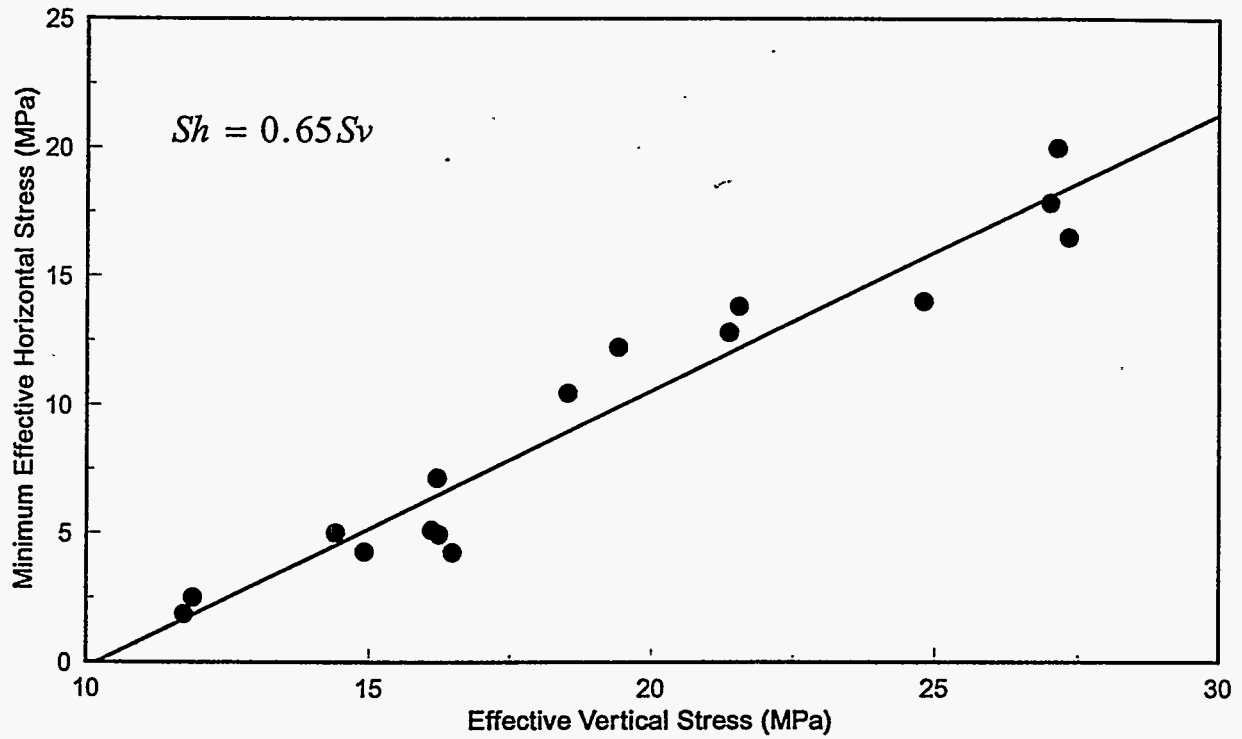
Mesaverde Sandstone

$$Sh = 0.65\,Sv$$

Figure 31. Plot of effective vertical stress versus minimum horizontal effective stress for the Mesaverde sandstone in the Rulison Field, Colorado.